The Operational Recognition of Supercell Thunderstorm Environments and Storm Structures

ALAN R. MOLLER

NOAA/National Weather Service Forecast Office, Fort Worth, Texas

CHARLES A. DOSWELL III

NOAA/Environmental Research Laboratories, National Severe Storm Laboratory, Norman, Oklahoma

MICHAEL P. FOSTER

NOAA/National Weather Service Forecast Office, Fort Worth, Texas

GARY R. WOODALL

NOAA/National Weather Service Forecast Office, Lubbock, Texas

(Manuscript received 24 May 1993, in final form 4 April 1994)

ABSTRACT

Supercell thunderstorm forecasting and detection is discussed, in light of the disastrous weather events that often accompany supercells. The emphasis is placed on using a *scientific* approach to evaluate supercell potential and to recognize their presence rather than the more empirical methodologies (e.g., "rules of thumb") that have been used in the past. Operational forecasters in the National Weather Service (NWS) can employ conceptual models of the supercell, and of the meteorological environments that produce supercells, to make operational decisions scientifically.

The presence of a mesocyclone is common to all supercells, but operational recognition of supercells is clouded by the various radar and visual characteristics they exhibit. The notion of a supercell spectrum is introduced in an effort to guide improved operational detection of supercells. An important part of recognition is the anticipation of what potential exists for supercells in the prestorm environment. Current scientific understanding suggests that cyclonic updraft rotation originates from streamwise vorticity (in the storm's reference frame) within its environment. A discussion of how storm-relative helicity can be used to evaluate supercell potential is given. An actual supercell event is employed to illustrate the usefulness of conceptual model visualization when issuing statements and warnings for supercell storms. Finally, supercell detection strategies using the advanced datasets from the modernized and restructured NWS are described.

1. Introduction

About 50 years ago it was observed that some tornadic thunderstorms moved to the right of the mean winds and contained a cyclonic circulation (Byers 1942; Brooks 1949). Two decades later, Browning (1964) presented a conceptual model that described the airflow within these storms, which he called "supercells." Interestingly, Browning's work was drawn primarily from volumetric radar reflectivity studies of two storms that occurred in geographically distant areas: Wokingham, England, and Geary, Oklahoma. Browning's model has survived with only minor modifications, but Doppler radar technology has made it possible to investigate the airflow within supercells directly and in far greater detail than Browning's original work. Dual–Doppler radar studies have revealed the three-dimensional structure of supercells (Ray et al. 1975), and three-dimensional numerical models have reproduced basic features of supercells and have helped explain important physical processes operating in these severe thunderstorms (Klemp 1987). The quantitative evaluation of physical processes (notably, the perturbation pressure distribution) made possible by numerical models has led to a revised supercell definition based on the presence of a strong correlation between vertical vorticity and vertical motion [i.e., a deep, persistent mesocyclone—see Weisman and Klemp (1984)].

Corresponding author address: Alan R. Moller, NOAA National Weather Service Forecast Office, 3401 Northern Cross Blvd., Fort Worth, TX 76137.

In general, no universally accepted definition of a mesocyclone exists, but the requirements used in development of operational mesocyclone detection algorithms have focused on vortex strength and space–time continuity of the vortex (Donaldson 1970). Thus, supercells are assumed herein to be those convective storms with mesocyclones; mesocyclones are assumed to have vertical vorticity greater than or equal to 10^{-2} s^{-1}, lifetimes at least on the order of tens of minutes, and are present through a substantial fraction (say, more than ⅓) of the convective storm's depth. While this definition is somewhat arbitrary, it appears to be capable of distinguishing significant storms from those that are much less likely to produce important severe weather.

Supercell storms are relatively rare; even during the spring months in the American Great Plains, only a small percentage of thunderstorms contain mesocyclones. Nevertheless, because of the severity of weather events that supercells produce, they result in a disproportionately large amount of thunderstorm-related casualties and damage. A sampling of 40 years of historical American supercell events was done to document the national scope of the supercell problem (Table 1). The cases were chosen to include the most significant events in terms of loss of life or property damage and also to reflect events in many different parts of the country.

Although supercells are most common in the central United States, they occur east of the Appalachians and even west of the Continental Divide. Many of the Table 1 events resulted in killer tornadoes, but it is intriguing that the two most damaging *nontornadic* severe thunderstorm events in U.S. history (*Storm Data,* July 1990 and May 1981) resulted from supercell storms, as verified in each case by Doppler radar indications of mesocyclones. The list in Table 1 is by no means complete, as thousands of other supercell events across the United States have resulted in deaths and extreme damage from downbursts, hail, flash flooding, and tornadoes. Supercells are a worldwide phenomenon and have been documented in England (the Wokingham storm, among others), France (Dessens and Snow 1989), and Australia (J. Colquhoun 1989, personal communication).

Table 1 suggests that supercell detection and subsequent warnings are of critical importance; unfortunately, supercells occasionally go undetected, especially at locations (and times of the year) where such events are infrequent. Indeed, where supercells are rare, a forecaster may go through an entire career without working a major supercell situation. Meteorologists in such areas often perceive that supercells and violent tornadoes do not occur there. Moreover, supercell detection has proven difficult when radar and/or visual storm structures deviate from what is perceived as the "standard" pattern (e.g., Moller 1978; Browning 1964; Fujita 1960). For supercell forecasting and detection, operational meteorologists need to know the pertinent meteorological questions to be asked and how to use scientific decision making rather than more empirical methodologies that have been used in the past. This

TABLE 1. Selected, notable supercell events.

Date	Location	Event(s)	Deaths	Supercell type	Tornado(es) visible?
11 May 1953	Waco, TX	Violent tornado	114	HP*	Yes
8 June 1953	Flint, MI, Cleveland, OH	Violent tornadoes	144	Classic	Yes
9 June 1953	Worcester, MA	Violent tornado	90	Classic	Yes
25 May 1955	Blackwell, OK, Udall, KS	Violent tornado	100	Classic	Yes
2 April 1957	Dallas, TX	Violent tornado	10	Classic	Yes
20 May 1957	Ruskin Hts., MO	Violent tornado	33	Classic	Yes
11 April 1965	IL, IA, IN, WI, MI, OH	Strong/violent tornadoes	258	Classic/HP	Yes
21 February 1971	MS	Violent tornadoes	113	Classic/HP	Yes
3 April 1974	East of Mississippi River from AL to MI	Strong/violent tornadoes	315	Classic	Yes
8 June 1974	OK, KS	Strong/violent tornadoes	22	HP/Classic	Yes
10 April, 1979	TX, OK	Strong/violent tornadoes	61	Classic	Yes
8 May 1981	Dallas/Ft. Worth, TX	Hail/wind storm ($250 million)	1	HP	—
28 March 1984	GA, SC, NC	Strong/violent tornadoes	57	HP	?
31 May 1985	OH, PA	Strong/violent tornadoes	65	Classic	Yes
28 February 1987	Laurel, MS	Violent tornado	6	HP	No
21 July 1987	Teton Park, WY	Violent tornado	0	HP (?)	?
11 July 1990	Denver, CO	Hail/wind storm ($500 million)	0	HP	—
13 March 1990	OK, KS, NE, IA, IL	Strong/violent tornadoes	2	Classic/HP/LP**	Yes
28 August 1990	Plainfield, IL	Violent tornado	28	HP	No
26 April 1991	OK, KS, NE	Strong/violent tornadoes	21	Classic/HP	Yes

* HP (high precipitation).
** LP (low precipitation).

paper will attempt to show that scientific decision making is inseparably linked to conceptual model recognition during supercell forecasting and/or nowcasting. Supercells will be considered within the context of a conceptualized thunderstorm spectrum, and then a supercell spectrum will be introduced for the purpose of aiding in supercell recognition. Atmospheric environments conducive to supercell formation will be emphasized, with physical reasoning again allowing us to develop conceptual meteorological models.

Much of the scientific literature concerns "classic" supercells (i.e., with highly visible storm-scale features such as wall clouds and tornadoes and clearly distinctive radar structures such as hook echoes), which will be described in detail below. Only recently has scientific investigation begun (e.g., Moller et al. 1990) on those supercells that have precipitation distributions that make them appear to be drastically different from classic supercells, at least in terms of visual and low-level radar echo characteristics. The occurrence of such storms that do not fit the classic model has caused considerable confusion in operational supercell identification.

An actual supercell event will be used to illustrate how conceptual model knowledge, as applied to multiscale diagnosis and forecasting, can lead to improved public statements and warnings for supercell storms. In this case study, only technology that is currently available to National Weather Service (NWS) field forecasters will be assumed. However, as part of our final discussion, we will propose some ideas about how the datasets expected to be available in the near future could be used to improve supercell forecasting and recognition.

2. Overview of the thunderstorm spectrum

Arrangement of storm types (and severe weather events) within the thunderstorm spectrum is based broadly on two ingredients: the buoyancy (i.e., convective available potential energy, or CAPE) and the character of the vertical wind shear. *Unorganized* convective storms generally are associated with low-shear, weak wind[1] environments, whereas high-shear, strong wind environments are usually characteristic of *organized* convection.

Unorganized storms typically are short lived (having a "pulselike" character), with new convective cells not developing in any consistent location relative to the cells preceding them. They may consist of one major cumulus tower (pulse storm) or a series of towers in close juxtaposition (unorganized multicell storm). Such storms as seen on radar can be isolated single cells but when seen visually usually consist of a series of updraft "bubbles." When such storms are seen on radar as *clusters* of cells, successive cells do not appear to follow their predecessors in any easily detected pattern, and the visual appearance of the cluster also reveals no obvious signs of organization. Outflows from dissipating cells interact in complex ways as each cell goes through its life cycle, and new cells develop in seemingly random ways, mostly as a result of these outflow interactions.

Increasing shear and instability leads to enhanced organization of the convection, with successive cells developing in preferred locations relative to their predecessors. New cell growth with organized multicell storms most frequently occurs on the right storm flank (relative to storm motion, in the Northern Hemisphere), with dissipating storm cells being shed on the left flank (Chisolm and Renick 1972; Marwitz 1972). Precipitation typically is thrown downwind by strong storm-relative winds aloft; with the storms moving slower than the mean wind in the storm-bearing layer, there can be considerable storm-relative wind near the storm top. Multicell line storms (squall lines) favor sequential cell development on the downshear (usually east) storm flank, mainly attributable to lifting along the long, nearly continuous gust front. Severe weather occurs as episodic events with organized multicell storms rather than as a quick burst of severe weather before dissipation, as is the case with unorganized pulse and multicell storms.

Real storms are hard to classify because convection is represented better as a continuous spectrum than as a collection of boxes with hard boundaries (Vasiloff et al. 1986). Many "hybrid" storms occupy the indistinct areas between more prototypical storms. The difficulties in classifying these hybrids and in determining the nature of severe weather that may occur with them make it critical that forecasters understand (and are able to modify) conceptual models of four-dimensional storm structure. This is particularly true of the hybrids between the supercell and nonsupercell categories, as described in the next section.

3. Overview of the supercell spectrum

It can be argued that the only scientifically supportable storm classification scheme is to categorize storms as either supercells or nonsupercells; the presence of a mesocyclone makes supercells dynamically different from other forms of convection (Weisman and Klemp 1984). In fact, because the operational definitions of severe weather are essentially arbitrary, it is apparent that *severe* versus *nonsevere* convection is not a scientifically valid distinction (see Doswell 1985). However, operational forecasters must make such distinc-

[1] It is rare to find a weakly sheared environment with uniformly strong winds in the vertical. Similarly, it is unusual to find a highly sheared environment with weak winds. Shear is more important, in general, to convection than the absolute wind speed, but observations support a connection between shear and speed.

tions anyway. Our aim in presenting the supercell spectrum herein is to assist in operational supercell recognition; there may be operational value in recognizing that supercells can take on a variety of radar and visual forms. We wish to enhance supercell *recognition* in this paper, not to proliferate new terminology.

a. *Supercell characteristics*

Supercell identification criteria historically have been applied in the absence of Doppler radar and/or volumetric reflectivity data. Most early U.S. Weather Bureau and NWS radar-based tornado warnings were issued after detection of low-level hook or pendant echoes. Historically, radar signatures used to issue tornado warnings have been derived purely empirically, including maximum reflectivities, echo-top heights, rotating storms (or mesoscale rotation of a group of storms), line-echo wave patterns (Nolen 1959), and V-shaped reflectivity notches. Such signatures generally have not been validated and so have only statistical relationships to tornado occurrence. In fact, four-dimensional storm *structure* (as seen on Doppler and/or reflectivity-only radars) is far more relevant than most of these empirical parameters (Lemon 1980; Imy et al. 1992).

Probably the most commonly cited supercell characteristic is that supercells are "steady-state" convective storms. Supercells as a group are indeed more nearly steady state than nonsupercell storms as a group; nevertheless, high-resolution radar invariably shows that supercell storms undergo a time evolution (along the lines described in Lemon and Doswell 1979). Further, a single supercell storm may well evolve through different parts of the supercell spectrum (to be presented below).

Another trait used to discriminate supercells is the notion that they are a single, continuous cell. This is not always the case, as some supercell storms have been observed to have multicell traits (Weaver and Nelson 1982; Vasiloff et al. 1986; Nelson 1987). Nelson's "multicell–supercell hybrid" may be simply a member of the supercell spectrum. Similarly, the so-called Westplains storm, which Foote and Frank (1983) place in a "hybrid" category between multicell and supercell, might fit somewhere within the spectrum presented below. It is our view that in determining whether or not a given storm is a supercell, its multicell traits are not important. A storm need not be unicellular to be a supercell; this is especially so for a storm that produces tornadoes cyclically, a situation that almost certainly involves a well-defined occlusion process (Burgess et al. 1982) and more than one cell.

Deviate motion (often erroneously taken to be to the right of the mean winds in the Northern Hemisphere) is another commonly used indicator of supercell behavior. However, if one were to limit supercells to those storms moving to the right of the mean winds, this would imply that a left-moving member (often the second member of a split pair) cannot be a supercell, even if it shows a persistent correlation between vertical vorticity and vertical velocity.[2] If the left-moving member in fact displays such a correlation, it clearly is a supercell. Also, the rightward motion is a result of updraft propagation, which may not always result in strong deviation in situations with strong tropospheric winds. While deviate motion may be an important clue that an intense and persistent storm is possibly a supercell, it is not definitive. Some nonmesocyclonic storms also move to the right (or the left) of the mean wind.

Lemon (1980) realized the difficulties in using only low-level signatures and range-height indicator scans to issue warnings (most notably, radar limitations and the inherent problems of low probability of detection and high false alarm rates), and suggested the *volumetric radar scan method,* which implies storm structure and updraft strength through the three-dimensional pattern of precipitation fallout around and/or through the updraft. Lemon's technique makes extensive use of radar-based thunderstorm structure research from both Alberta, Canada (Chisolm and Renick 1972), and Oklahoma. In essence, Lemon proposed an operational methodology for tornadic storm detection using radar reflectivity information alone, stepping up from the *associative* (is a hook-shaped echo present?) to the *scientific* (is the three-dimensional reflectivity structure consistent with what is known about supercells?). Lemon's notion of supercell characteristics uses the full three-dimensional reflectivity morphology and its temporal evolution. While nothing is more unambiguous in supercell detection than the observed presence of a deep, persistent mesocyclonic flow, the Lemon criteria, such as Bounded Weak Echo Regions (BWERs), are very good indicators. Thus, for example, it is extremely unlikely that a convective storm with a bona fide BWER would turn out to not have a mesocyclone (D. Burgess 1990, personal communication). However, not every storm with a mesocyclone has a BWER.

We continue to endorse the three-dimensional view of convective storms embodied in Lemon's conceptual models, and so we echo the position of Imy et al. (1992), advocating the use of volumetric reflectivity data whenever possible. Our intent in this paper is to provide those operational meteorologists accustomed to using only low-level reflectivity data with encouragement to use volumetric radar scans in searching for

[2] When dealing with the left-moving member of a split pair (in the Northern Hemisphere), the correlation between vorticity and updraft will be *negative,* since the updraft is rotating anticyclonically.

severe convection and to give information that should help them identify potential supercells since supercells include a broader range of reflectivity structures than is commonly recognized (Doswell et al. 1990).

b. Classic supercells

Most supercell studies, from Browning's so-called Geary storm to those in the recent past, have been drawn from the transitional environment[3] of the southern Great Plains (moderate to high moisture, with intermediate level of free convection values (LFCs), often with a preconvective capping inversion). These storms frequently comprise relatively isolated convection, developing well apart from competing storms. They have the well-known radar signatures, such as a hook- (or pendant) echo structure revealed in relatively low reflectivity [i.e., NWS Video Integrator and Processor (VIP) levels 2 or 3, corresponding to 31–40- and 41–45-dB*Z* reflectivities, respectively]. Radar reflectivity volume scans typically show a BWER and storm-top displacement to above the low-level pendant (Chisolm and Renick 1972; Lemon 1980).

Visually, classic supercells often exhibit upshear flanking convective lines with apparent precipitation-free bases and a well-defined lowering [called a "wall cloud" (Fujita 1960)] from which tornadoes descend (Fig. 1). Note that while the updraft base may be rain-free visually, scattered hail and raindrops may be falling in this area, creating thin "curtains" of precipitation that may rotate around the mesocyclone (seen on radar as the hook echo). Moreover, even at its lowest elevation, the radar beam may be far enough above ground level to be slicing the storm well aloft, where most precipitation particles are suspended by updraft in the pendant area of the cell. Our interpretation of the data presented in the literature for several of the great tornado outbreaks since 1950 (e.g., Penn et al. 1955; Fujita et al. 1970; Forbes 1981; *Storm Data,* May 1985), as well as evidenced in Environmental Science Service Administration/National Oceanic and Atmospheric Administration disaster survey reports, is that major outbreaks are dominated in numbers by classic supercells.

c. Low-precipitation supercells

Mid-1970s thunderstorm intercept teams first noted that some storms did not have all the classic radar characteristics but could be visually spectacular in revealing rotation (see, e.g., Burgess and Davies-Jones 1979). These storms came to be known as low-precipitation (LP) supercells (Bluestein and Parks 1983).

[3] The transition involved is that between the typical high-moisture environment of the Mississippi Valley and the low-moisture environment of the high plains.

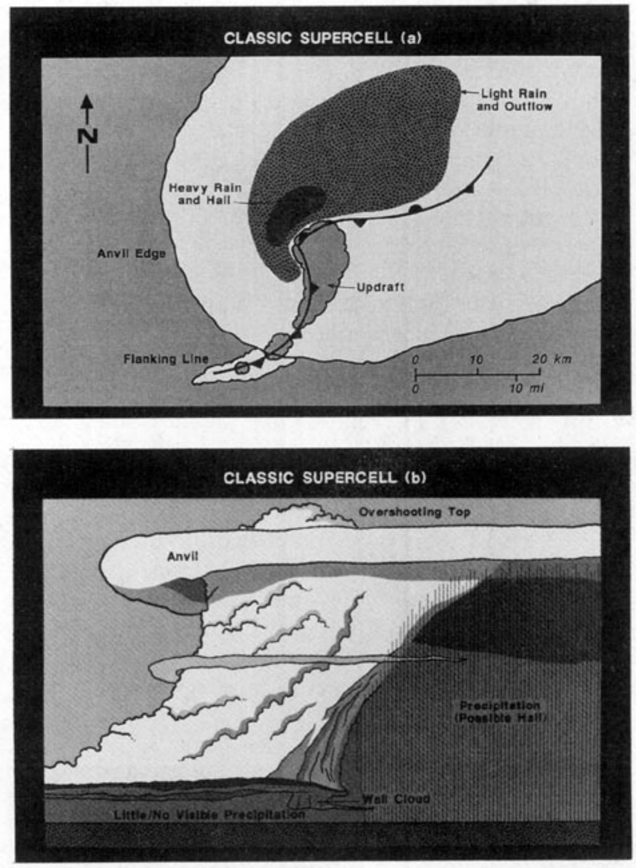

FIG. 1. Schematics for a classic supercell storm, showing (a) a plan view looking from above showing the precipitation (stippling), surface outflow boundaries (frontal symbols), updraft maxima (scalloped line), and cloud boundaries (also scalloped), and (b) an idealized view of the storm by a surface observer to its east.

Such storms are virtually unique to the surface dryline environment, mainly the high plains east of the Rocky Mountains and western portions of the Great Plains. Low-precipitation storm environments are characterized by low-to-moderate moisture values and relatively high LFCs. Capping inversions, if present, erode quickly in the vicinity of the dryline, and so deep convection typically develops first near the dryline. Low-precipitation storms can appear benign on radar, often exhibiting low reflectivities despite producing large hail. Such storms have been simulated numerically by the artifice of preventing liquid precipitation in a three-dimensional cloud model (Weisman and Bluestein 1985) and also by initiating the model with a smaller-than-normal buoyant "bubble" (Brooks and Wilhelmson 1992). These simulated LP storms bear a striking resemblance to observed storms, tending to be smaller in diameter than classical supercells, which may explain the observed low radar reflectivities in the presence of large hail: a small storm may not fill the beam. Given the high cloud bases and limited precipitation, trained storm spotters are of considerable value in recognizing LP supercells, because using radar reflectivity alone usually proves ineffective.

Severe weather with LP storms usually is limited to large hail and only occasional tornadoes. Violent tornadoes, although rare in any case, are quite unlikely with LP storms; to date, none has been observed to occur with a bona fide LP supercell. The lack of significant rain precludes much chance for damaging outflow winds and flash flooding. A detailed analysis of an LP storm by Bluestein and Woodall (1990) suggests the absence of a significant outflow and associated gust front, which appears to be typical for LP storms (see also Burgess and Davies-Jones 1979). Figure 2 summarizes LP supercell features.

d. High-precipitation supercells

Whereas LP storms exhibit little or no precipitation (and low reflectivity) in the mesocyclone, "high- (or heavy) precipitation" (HP) supercells are characterized by substantial precipitation in the mesocyclone. There are several paths by which a mesocyclone comes to be embedded in substantial precipitation. One of the ways

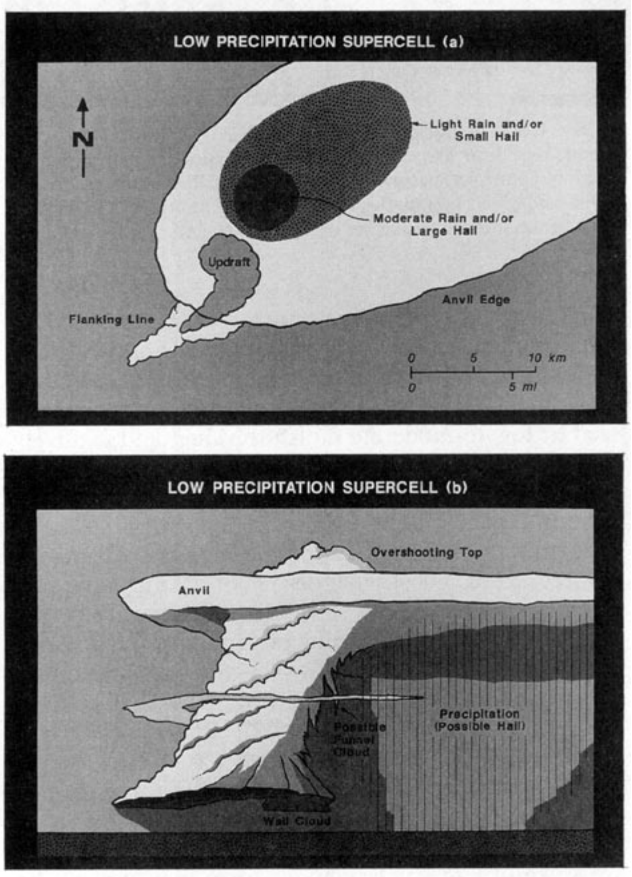

FIG. 2. As in Fig. 1 except for an LP supercell storm.

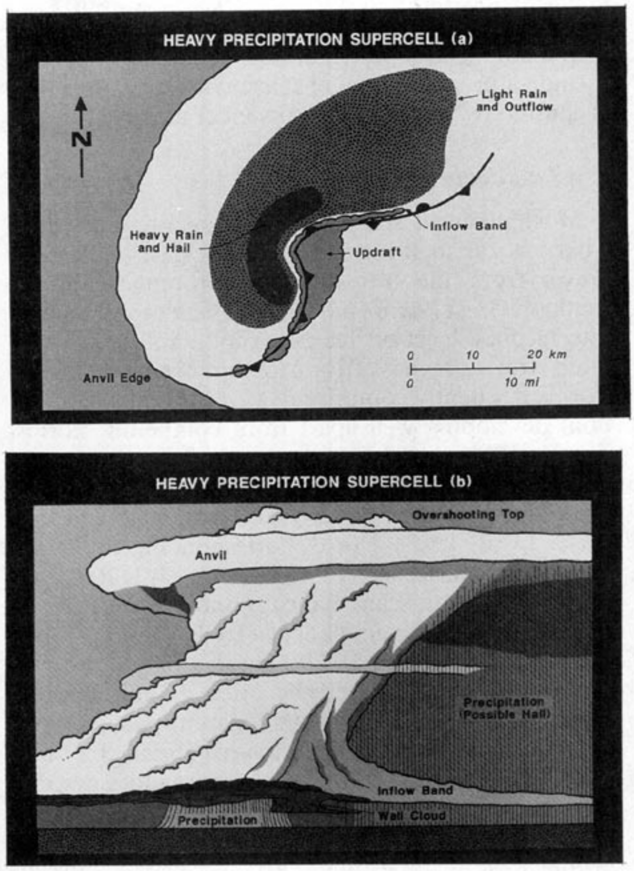

FIG. 3. As in Fig. 1 except for a heavy- (or high) precipitation supercell storm.

in which this occurs is associated with the central plains of the United States during the warm season, and it often is possible for human observers to see distinctive visual characteristics (e.g., Fig. 3). Such structures may evolve from classic supercells (Fig. 4), and in some situations, the evolution from classic supercell results in a bow-echo structure. In still other cases, the evolution becomes complex and there is no clearly distinctive echo morphology. As the mesocyclone moves with respect to the precipitation, inflow notches, spiral bands, and other complicated reflectivity structures can arise (see Johns and Doswell 1992; Przybylinski 1988; Przybylinski et al. 1990). At least some of this spectrum of supercell structure that includes HP-like storms has been simulated numerically by Weisman and Klemp (1986). The key, of course, is the presence of a mesocyclone, which can be determined most unambiguously with Doppler radar, and then only provided the storm is close enough to the radar.

Not all such supercells occur in the warm season on the plains. When cool season events arise, it is common for them to be quite difficult to recognize visually, owing to low cloud bases and extensive intervening clouds

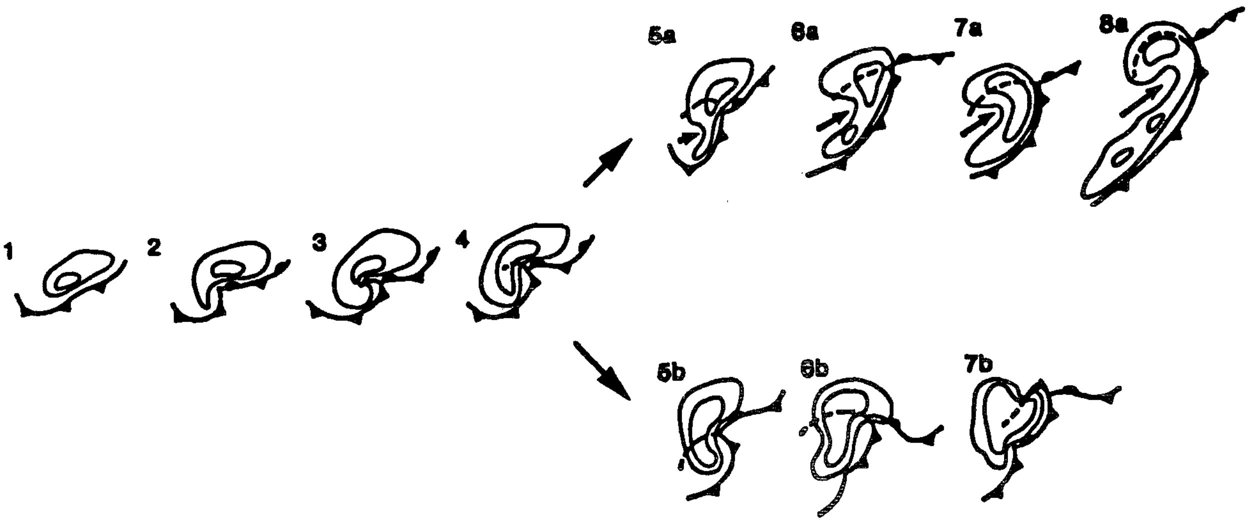

FIG. 4. Schematic showing two different paths of evolution with HP supercells, adapted from Moller et al. (1990). The low-level reflectivity patterns are shown as thin solid lines, and the associated outflow boundaries are depicted with frontal symbols. The "a" sequence (upper right) shows the rear downdraft/outflow with small arrows.

common to regions of the United States outside of the central and western plains.[4] Moreover, radar detection of such events can be quite difficult because storms in the cool season often have low tops (Vescio et al. 1993), so the radar (even a Doppler radar) may "overshoot" the relevant storm structural details.

Moller et al. (1990) have presented a preliminary conceptual model for this supercell type. It appears that the HP storm is the dominant form of supercell, nationwide (Johns et al. 1993). As noted above, we believe outbreaks of tornadoes are dominated by classic supercells. However, a significant fraction of these storms appears to have been HP supercells. (Some may have undergone transition from classic to HP supercell—Table 1.) In fact, a given storm may exhibit LP, classic, and HP characteristics during its lifetime (Bluestein and Woodall 1990).

By having mesocyclones thoroughly embedded in precipitation, those HP supercells that *do not* evolve into bow-echo configurations can resemble classic supercells that are in the throes of mesocyclone collapse (see Lemon 1980; Lemon and Doswell 1979). High-precipitation storms differ, however, by maintaining this structure rather than by simply dissipating. Radar volume scan strategies (such as the Lemon technique) will reveal supercell storm structural features (e.g., BWERs) successfully, assuming that forecasters recognize that HP storms may exhibit their mesocyclones closer to the front flank (relative to storm motion), and so the forecaster is looking at the right places within the echo. The chances of looking in the right place of an echo are greatly improved by performing volume scans (see Imy et al. 1992).

Those HP storms that *do* develop bow-echo structures are not as isolated from surrounding convection as LP or classic storms, although they may remain "distinctive" (Forbes 1981) in character (see, e.g., Fig. 4). Furthermore, they may not have reflectivity morphologies aloft (e.g., BWERs) that make them easily recognizable as supercells, in spite of the presence of a mesocyclone. Misidentification can occur not only because of neighboring storms but also from precipitating convection along the supercell's rear-flank downdraft (RFD) gust front and, occasionally, from radar reflectivity pendants along convergence lines in the low-level storm inflow field (such storms may have multiple flanking lines).

Clearly, the abundance of precipitation in and near the HP storm's mesocyclone makes for difficult, and occasionally hazardous, storm spotting. The lack of conspicuous visual characteristics makes it difficult to provide an example of a bow-echo configuration HP supercell comparable to that shown in Fig. 3b, and so we have not done so. Forecasters should understand that not every HP supercell is going to match exactly the reflectivity pattern shown in Fig. 3a; Fig. 4 attempts to provide some examples of variations on the echo morphology but should not be considered exhaustive of what one might see in a given situation. What is important is to recognize the tornado potential of storms whose structure suggests mesocyclonic rotation and to understand that radar may not detect those structures in every case. This is especially problematic

[4] Such difficulties also arise in the plains, of course.

when the storms have low tops and/or are relatively far from the radar. In a very real sense, the HP supercell category is being used as a "catchall" for any storm that has a deep, persistent mesocyclone embedded in precipitation, and so the variety of structures is potentially confusing. This topic certainly deserves further study; therefore, we are attempting to provide operational forecasters with some guidelines to recognize threatening events, not to define the HP supercell category's precise boundaries.

Although HP supercells apparently do not produce strong and violent tornadoes as often as classic supercells, they are still dangerous storms (see, e.g., Moller et al. 1990). Further, HP storms can produce torrential rainfall, posing a significant flash flood threat in addition to the severe weather risk. Concerning hail and downbursts, some of the worst severe weather events in U.S. history have occurred with HP storms (Table 1). Severe weather production in HP storms often occurs over relatively long and broad swaths (Moller et al. 1990). This suggests that derecho-producing storm events (Johns and Hirt 1987) may include HP supercell storms as part of the mesoscale storm complex.

e. Supercell environments

Forecasters who understand the meteorological processes that produce supercells are less likely to be surprised when mesocyclonic storms form. Initial tornado forecast studies resulted in empirical forecast rules that focused on the role of highly baroclinic, synoptic-scale systems (Miller 1972). Recent research has shown that such easily recognized disturbances are not always present with supercell storms (e.g., Maddox and Doswell 1982). Furthermore, when such a disturbance does accompany severe weather, it appears that its main contribution is not to serve as a convective "trigger" (synoptic-scale vertical motions on the order of several centimeters per second^{-1} usually are not sufficient to initiate convective storms) but to destabilize the thermodynamic structure and to increase the vertical wind shear (Doswell 1987).

The lift needed to initiate deep, moist convection then is provided by mesoscale or storm-scale processes (e.g., drylines, stationary fronts, warm fronts, and outflow boundaries from previous storms). Increased low-level, vertical wind shear from locally backed surface winds along thermal boundaries (e.g., warm fronts, outflow boundaries, etc.) appears to aid supercell development in many cases (Maddox et al. 1980). This appears to be particularly important for many HP-type supercells (Moller et al. 1990).

In section 2, we stressed that the main determinants of convective storm type within the storm spectrum are buoyancy (CAPE) and vertical wind shear. Numerical models (Weisman and Klemp 1982, 1984, 1986; Klemp 1987) and observations (Chisolm and Renick 1972; Fankhauser and Mohr 1977; Burgess and Curran 1985) show that vertical wind shear is the most crucial of these two parameters for supercell development. More specifically, certain patterns of vertical wind shear allow the storm updraft to tilt existing horizontal vorticity (arising from the vertical wind shear) into the vertical. The resulting helical updraft (helical in a storm-relative streamline sense) is seen as a mesocyclone.

Numerical modeling results and observations also agree that, given a certain fixed amount of buoyancy, convective storm persistence increases with the vertical wind shear (at least to some ill-defined limit, beyond which intense shears become destructive to convection). A natural question concerns the role of CAPE in supercells; at the time of this writing, this question remains unanswered except that some CAPE is needed in any deep convective storm. During the warm season over the plains, high lapse rates can develop over the Mexican Plateau (Carlson et al. 1983) and the east slopes of the Rocky Mountains (Doswell et al. 1985). When a traveling disturbance advects these high lapse rates over an area of abundant low-level moisture, the classical capped, "loaded gun" sounding associated with severe weather is created. Thus, supercells in the plains during the warm season often have relatively high CAPE and, in major outbreaks, the wind shear is associated with the highly baroclinic weather systems already mentioned.

However, not all supercells arise this way. As noted in Johns and Doswell (1992), a substantial fraction of supercells nationwide arise in situations with CAPEs less than 1500 J kg^{-1} (see, e.g., McCaul 1991; Braun and Monteverdi 1991). Although we do not yet understand the complex interaction between CAPE and vertical wind shear in real storms, it is important for forecasters to realize that the absence of high CAPE does not exclude the possibility of supercells. At times, damaging supercells occur with low CAPEs [e.g., the northern Indiana tornadoes of 3 April 1974 and the Raleigh, North Carolina, tornado of 28 November 1988 (Korotky 1990)].

Johns (1993) has examined the environments associated with bow-echo events and found that directional shear tends to be less in bow-echo storms than in classic supercell environments. Since the bow-echo structure can evolve out of more classical supercell morphologies (and vice versa), it is logical to suggest that the storm structural changes can result from storms moving into different environments. Burgess and Curran (1985) present a case where storm structure changes when moving into an environment with substantially different vertical wind shear. [Alternatively, Weisman (1993) shows in a numerical model that storm structure transition may represent a natural evolution within a given environment.] Brooks et al. (1994) have indicated that the relationship of a me-

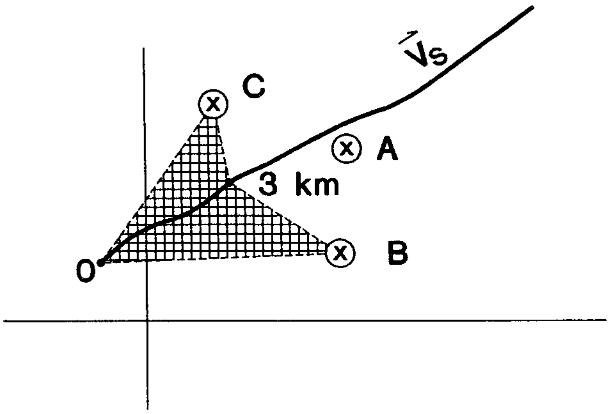

FIG. 5. A schematic straight-line hodograph, showing the initial storm motion (circled "X" labeled "A"), and after the storm splits into a right-moving ("B") and a left-moving member ("C"), with the hatched areas showing the area corresponding to the 0–3-km storm-relative helicity.

socyclone to the precipitation is determined by the storm-relative flow at midlevels. Clearly, much remains to be understood about the environments associated with the spectrum of mesocyclonic storms.

Nevertheless, there is general agreement that supercell environments are associated with the spatial and temporal limits of two elements: 1) deep, moist, and persistent convection,[5] and 2) vertical wind shears conducive for mesocyclones. Clearly, severe weather–producing mesocyclones are not likely in the absence of deep, moist convection.

Given the presence of deep, moist convection, the vertical wind shear of greatest importance for mesocyclone formation appears to be in the convective storm's inflow layer, generally limited to the lower 3 or 4 km of the atmosphere. No "magic" values of low-level wind shear characterize the supercell environment. Weisman and Klemp (1982, 1984) have proposed that shear and buoyancy be combined into a single parameter, the so-called bulk Richardson number (BRN), also denoted by Ri, where

$$\mathrm{Ri} \equiv \frac{\mathrm{CAPE}}{\frac{1}{2}(\bar{u}^2 + \bar{v}^2)}, \qquad (1)$$

with u and v representing the components of the vector difference between the density-weighted mean wind over a 6-km depth and a representative surface layer (lowest 500 m) wind. The shear used in the denominator of (1) at times is referred to as the "BRN shear" (as in Droegemeier et al. 1993). Weisman and Klemp (1986) suggest that Ri values between 10 and 40 favor supercells and that BRN shears $<3 \times 10^{-3}\ \mathrm{s}^{-1}$ define "weak" shears (too weak to provide substantial organization to the convection).

While BRN has predictive value in anticipating supercells, there are only surface-based observations available to update CAPE between soundings. Furthermore, experiments conducted jointly by the National Severe Storms Laboratory and the National Weather Service in Norman, Oklahoma, have shown storm-relative environmental helicity (SREH), another measure of mesocyclone potential, to be a most useful operational forecasting tool (Davies-Jones et al. 1990, hereafter DBF90). If H denotes SREH, then

$$H \equiv -\int_0^h k\cdot(V - C) \times \frac{\partial V}{\partial z}\, dz, \qquad (2)$$

where k is the unit vector in the vertical, V is the horizontal wind vector, and C is the storm motion vector, while h is an assumed inflow-layer depth, typically 3 km.

New technologies like vertical wind profilers and WSR-88D Velocity-Azimuth Display (VAD) winds can be used to update SREH estimates many times during the day. SREH can be found from a hodograph as minus twice the area swept out by the storm-relative wind vector in the lower 3 km of Figs. 5 and 6 (as described in DBF90). Helicity calculations already are available in PC-applicable form, either for single-station analysis (DBF90; Korotky 1990) or on a regional map (Woodall 1990). It is important to note that while helicity currently is becoming widely used in determining supercell potential operationally, it is subject to rapid temporal and spatial changes. Meteorologists must attempt to update helicity values based on numerical model forecast data and changes in local surface winds, profiler data, Doppler radar data, and/or radar-indicated storm motion. A shear structure favorable (unfavorable) for mesocyclone formation may change quickly to a nonsupercell (supercell) atmosphere (Burgess 1988).

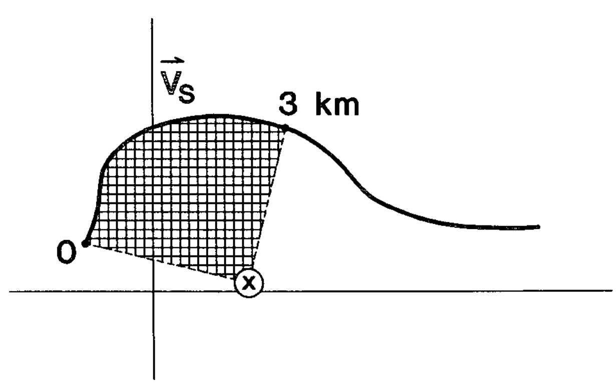

FIG. 6. A schematic curved hodograph, showing a typical storm motion (circled "X"), with the hatched area as in Fig. 6.

[5] Deep, moist convection, in turn, has three primary ingredients: moisture, instability, and lift (see Johns and Doswell 1992).

Davies-Jones et al. (1990) have suggested helicity values ($m^2 s^{-2}$) for weak, strong, and violent tornadoes of 150–299, 300–449, and greater than 450, respectively. Forecasters should be aware that the values started by DBF90 are subject to a number of caveats (Doswell and Brooks 1993): they are only preliminary, having been based on a small sample, and helicity's role in supercells and tornadoes is still being investigated. Limited operational experience in using helicity has taught us that when current or projected helicity values exceed a value somewhere around 100–150 $m^2 s^{-2}$, supercells are quite possible. The higher the helicity, the greater the supercell potential. Tornadoes, on the other hand, are *not* as clearly related to helicity (see Brooks et al. 1994), although the chances for strong and violent tornadoes increase as supercell potential increases.

Generally, mesocyclone potential is high when the low-level winds are strong (Droegemeier et al. 1993), the hodograph (vertical wind shear vectors) veers with height, and storm motion is well to the right of the mean environmental wind (Fig. 6). However, numerical simulations have demonstrated that a straight-line hodograph (Fig. 5) also can produce supercells when atmospheric winds (and, more importantly, wind *shears*) are generally strong; in some such cases, the initial storm's motion (vector A in Fig. 6) is along the mean wind vector. This initial storm then splits into two cells that are nearly mirror images of one another (Schlesinger 1980; Weisman and Klemp 1982, 1986). The model simulations indicate that straight-line hodographs produce a cyclonic–anticyclonic vortex pair on the flanks of the initial updraft. This structure promotes new updraft development of the flanks through perturbation pressure forces. This, in turn, favors movement off the hodograph by propagation. The right-moving member (vector B) rotates cyclonically, whereas the left-moving member moves to the left of the environmental mean wind (vector *C*) and rotates anticyclonically. Theoretically, in an atmosphere with a straight-line hodograph, neither of the pair is favored and both storms tend to persist. Real storms have exhibited this sort of behavior (see Charba and Sasaki 1971). Thus, forecasters should recognize that even in straight-line hodograph situations any storms having a motion vector *off the hodograph* can have significant storm-relative helicity (Doswell 1991). Those that do have high helicity are likely to be supercells. Another way for storms to move off the hodograph (thereby enhancing their storm-relative helicity) besides storm splitting is for storm motion to be influenced by external mesoscale processes and/or terrain features (see Maddox et al. 1980; Imy et al. 1992; Doswell 1985, Fig. 3.8a,b).

When the hodograph curves clockwise with height, as in Fig. 6, the right-moving member is favored over the left-moving member (Weisman and Klemp 1984). Moreover, storm motion in environments with curved hodographs is virtually never on the hodograph, and therefore, it is relatively easy for most storms to have substantial storm-relative helicity (Doswell 1991). Of course, one must actually do the helicity calculations; a suggested method is to put contours of SREH directly on the hodograph (as in DBF90), thereby providing an instant estimate of SREH for any storm motion. Having a motion inside a curved hodograph does not guarantee supercell storms, but if the resulting SREH is large, then the chances for a supercell are correspondingly high. Many observations (e.g., Browning 1964; Chisolm and Renick 1972) show that the most intense supercells (and violent tornado situations), with a few notable exceptions, favor the clockwise curved hodograph.

There are indications that low-level wind shear structure may not tell the whole story (Brooks et al. 1993). While parameters based solely on the low-level part of the wind profile seem to offer considerable help in delineating supercell environments, it appears that they do not "close the book" on the forecast problem. In particular, getting a strong mesocyclonic circulation at or near the surface may require more than strong helicity in the inflow layer. Recent modeling work (Brooks et al. 1994) suggests that midlevel storm-relative wind is a key factor in producing low-level mesocyclones and, hence, increasing tornado potential. According to Brooks et al., weak midlevel storm-relative winds result in a modeled storm resembling an HP supercell. A large amount of precipitation falls close to the updraft, apparently helping to spin up the low-level mesocyclone through baroclinic generation of vorticity in the downdraft. However, the cold-air outflow undercuts the storm's inflow, cutting short the duration of high vertical vorticity in the low levels. When midlevel storm-relative winds are increased, more of the rain falls away from the updraft. In this case, baroclinic generation of vorticity in the RFD is slower but the high vertical vorticity phase is more persistent. These results suggest that whereas low-level vertical wind shear techniques are essentially predicting *supercells,* consideration of a deeper layer of vertical shear may be needed to forecast *tornadoes.*

4. The supercell case of 4 May 1989

We wish to exemplify how the preceding concepts might be used operationally, in a chronological simulation of a real-time forecast event. In doing so, we shall provide examples of products that *might* have been generated on the day in question but that do *not* represent the actual products issued. For our purposes, the actual forecast and warning products produced by the NWS Forecast Office (NWSFO) at Fort Worth, Texas, are not important; our idea is to show what *could* be done using the ideas we have developed, not

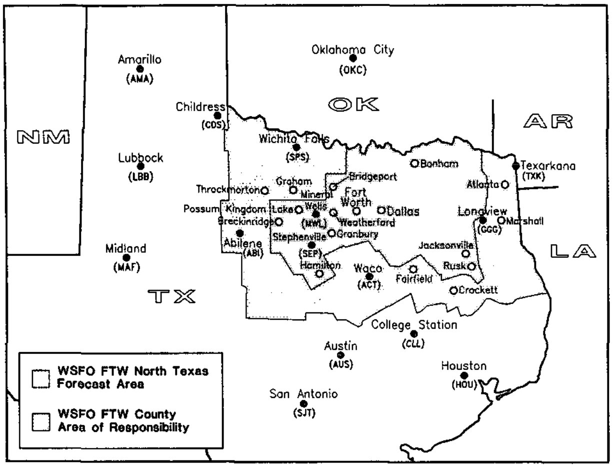

FIG. 7. Map showing the location of towns mentioned in the text and selected observation sites (labeled with three-letter identifiers). The light stippling covers the Weather Service Forecast Office (WSFO) Fort Worth, Texas (FTW), north Texas Forecast Area, while the heavy stippling covers the WSFO Fort Worth County Area of Responsibility (CAR).

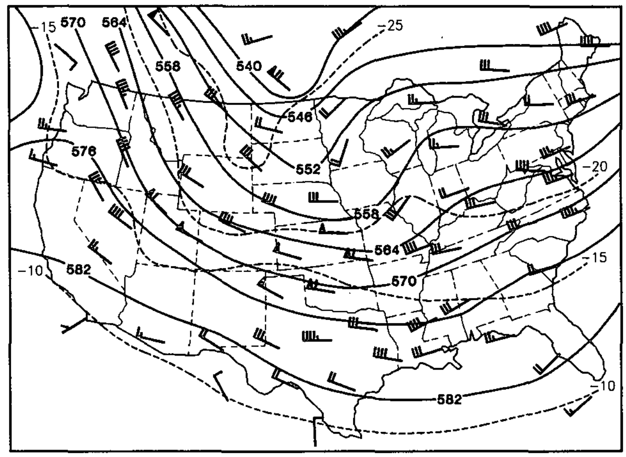

FIG. 8. The 500-mb analysis chart valid at 1200 UTC 4 May 1989, showing heights (solid lines, decameters) and isotherms (dashed lines, degrees Celsius), with conventional wind barbs plotted at the available sounding sites.

to second guess the forecasters who dealt with the event in real time.

A series of thunderstorm complexes moved southeast across north Texas (NWSFO Fort Worth's forecast area, see Fig. 7) in the period from 2 May 1989 through early 5 May 1989. The last of these events produced widespread severe weather during the evening of 4 May and the early morning of 5 May (Smith 1990). We have selected this case because the short-range prediction and detection of supercell occurrence were difficult (as they often are). Furthermore, different modes of supercell storm apparently occurred (i.e., although there was not direct Doppler evidence of mesocyclones, radar structures and attendant weather events strongly indicated the presence of both classic and HP supercell storms) within a derecho-producing bow-echo complex. A warning forecaster could easily miss the details of these storm-scale supercell structures in the presence of such a distinctively shaped mesoscale convective system.

In the process of a multiscale meteorological diagnosis, we shall formulate proposed Severe Weather Outlook (SWO) statements that are short-range severe storm forecasts for emergency preparedness officials, spotters, and the news media.[6] Finally, we shall generate simulated severe weather statements that emphasize the particularly dangerous supercell threat to the general public.

The synoptic weather pattern included cyclonically curved northwest flow aloft (Fig. 8) and a nearly stationary frontal boundary oriented parallel to the mid-level wind field (Fig. 9). There was strong low-level warm thermal advection and moisture convergence along the front and outflow boundaries from the morning storms, indicating both large-scale and mesoscale sources of ascent. The upper flow was west-northwesterly, while moderate southerly low-level flow

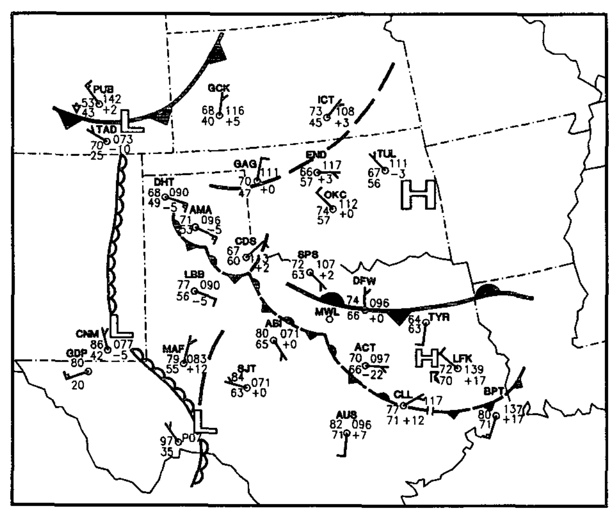

FIG. 9. Surface analysis at 1800 UTC 4 May 1989, showing selected surface observations [standard plotting model, showing temperature and dewpoint temperature (°F), sea level pressure (mb—conventional abbreviation), and 3-h pressure tendency], and important boundaries. Large frontal symbols denote conventional frontal boundaries; small, dashed frontal symbols denote outflow boundaries; dashed lines denote troughs; and scalloped lines denote the dryline. See Fig. 8 for three-letter identifiers of surface observation sites.

[6] The National Weather Service Forecast Office, Norman, Oklahoma, pioneered SWOs in the mid-1980s, calling their product the Oklahoma Thunderstorm Outlook. Since then, Fort Worth (FTW) and other nearby offices have used the product.

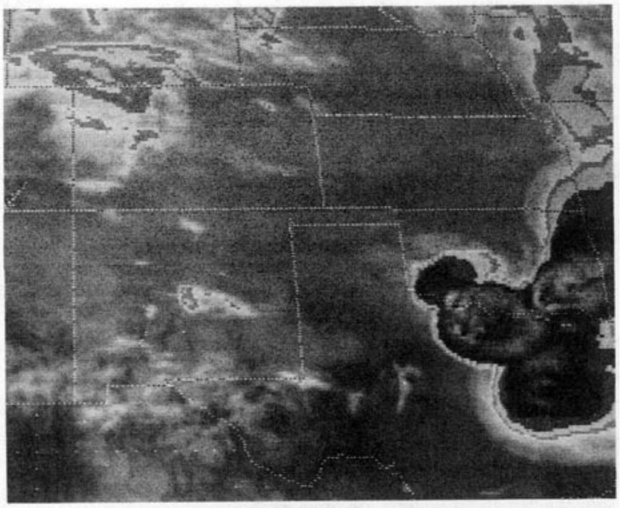

FIG. 10. Enhanced infrared GOES image at 1001 UTC, showing severe thunderstorms across the north Texas area.

was advecting dewpoints in excess of 70°F (21°C) toward the surface boundaries. It is well known (e.g., Miller 1972) that this basic synoptic pattern can be favorable for severe convection.

Given this morning setting, and knowing that a series of midlevel short-wave troughs was embedded in the upper-air flow, it is reasonable for a forecaster to be concerned with a severe weather and tornado threat. Knowledge of the timing, character, and intensity of these short-wave troughs is always a difficult forecast problem, but in the wake of the morning convection, a quite threatening environment could be created from the basic ingredients already present.

Our forecast begins at 0500 CDT (1000 UTC) on 4 May. Widespread thunderstorm activity is present at this time (Fig. 10), with severe thunderstorm, tornado, and flash flood warnings having been issued as the thunderstorm complexes moved through north Texas. There is no question that southeast sections of the forecast area will have a threat of severe weather during the next several hours due to the existing storms but we must ascertain the severe weather threat beyond that time frame and area. Although the 1200 UTC instability[7] and 0–3-km helicities (Fig. 11) appear favorable for supercells at this time, it appears that the threat could be reduced substantially by the stabilizing effects (low-level cooling, moisture depletion, and a decrease of lapse rates) of the widespread morning convection. The 1200 UTC hodograph's strong low-level helicity[8] clearly is being affected by the nocturnal low-level wind maximum, which is likely to decrease as the day opens (see Maddox 1993). Thus, it appears that additional processes later in the day may be needed to reestablish atmospheric conditions conducive for severe storms. Owing to the premature termination of the sounding, the BRN could not be calculated.

The 12-h forecast from the nested grid model (NGM) valid at 0000 UTC 5 May 1989 (Fig. 12) is in close agreement with the previous 24-h prognosis (not shown) in the depiction of a midtropospheric disturbance approaching north Texas during the evening. These forecasts are supported by the morning satellite images (Fig. 10) showing a short-wave trough–associated cloud mass near the Colorado–Wyoming border

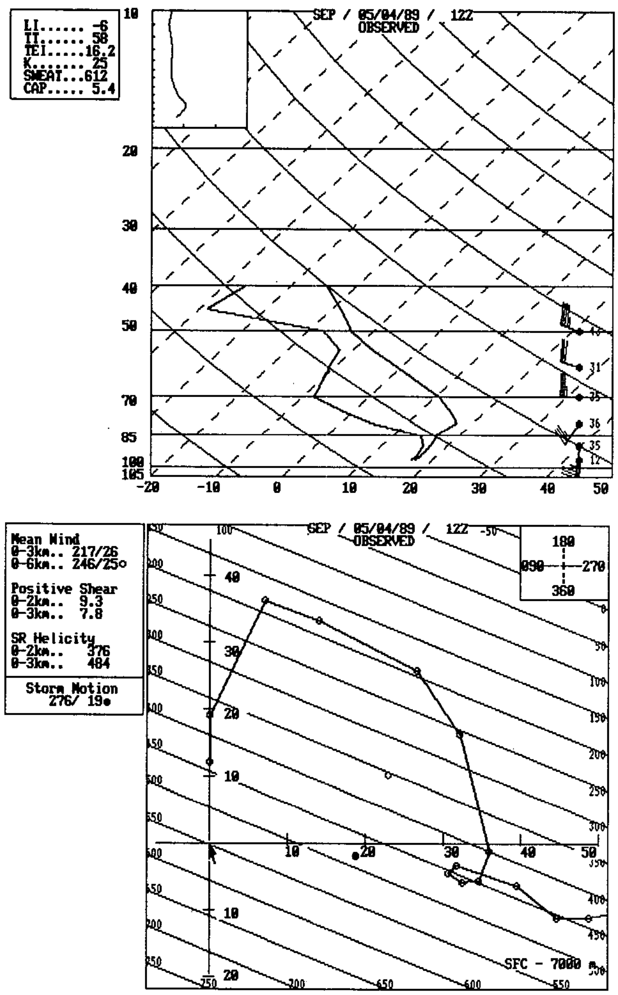

FIG. 11. Stephenville sounding at 1200 UTC 4 May 1989, showing (a) the temperature (solid) and dewpoint (dashed) traces plotted on a skew T–log$p$ diagram, and (b) the hodograph (line connecting open circles, depicting the wind profile at 200-m intervals), with contours of storm-relative helicity ($m^2 s^{-2}$) as the sloping thin lines. In (b) the hodograph coordinates are in knots. The lifted index was calculated using the "PMAX" method of the SHARP workstation (Hart and Korotky 1991).

[7] The sounding was terminated near 400 mb, so CAPE could not be computed. The lifted index, however, was −6 at 500 mb.

[8] The helicity values are *storm relative,* using the SHARP program's technique for estimating storm motion to be 30° to the right of the mean wind, at 75% of its speed.

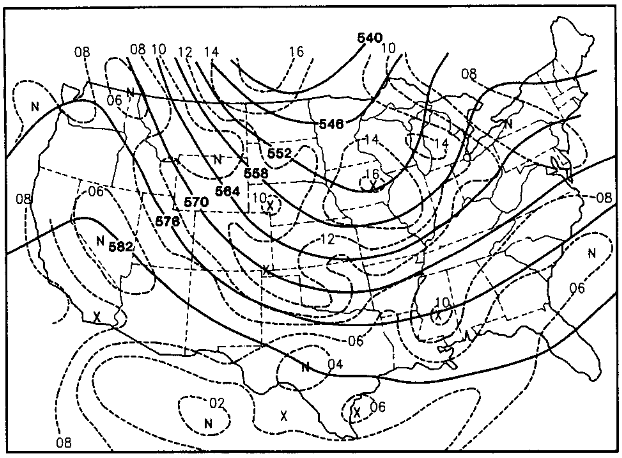

FIG. 12. The 500-mb NGM forecast valid at 0000 UTC 5 May 1989, showing height contours (solid lines, decameters) and absolute vorticity (dashed lines, with values times $10^{-5}\ s^{-1}$). Vorticity maxima are denoted with a large "X," and minima by the large "N."

area. The consistency between the observed data and the successive NGM forecasts indicates that destabilization due to the short-wave trough's vertical motion can be expected across north Texas late in the afternoon or evening, renewing the threat of thunderstorms. However, both the aerial coverage and potential severity of these storms is in question at this time.

By 1800 UTC, very light winds on surface charts (Fig. 9) and NGM-based wind forecasts (not shown), which have the low-level jet stream shifting eastward into Louisiana, plus the normal decrease in speed expected during the day, all indicate light winds through the lowest 3 km over north Texas during the afternoon and evening. Thus, afternoon and early nighttime helicity values may not be as high as those on the 1200 UTC Stephenville (SEP) sounding. Furthermore, Fig. 9 and computed surface moisture convergence fields (not shown) reveal that the strongest moisture convergence is near a thunderstorm outflow boundary in extreme southern portions of the forecast area at 1800 UTC. On the chance that the approaching short-wave trough will increase the midlevel lapse rates (which probably have been reduced by the morning thunderstorms) and cause the outflow boundary to move northward somewhat, a severe weather statement for both the existing severe weather and severe weather potential might read as follows.

Severe Weather Outlook Statement
National Weather Service Forecast Office, Ft. Worth
Issued: 12 Noon CDT Thu May 4 1989

A severe thunderstorm warning remains in effect for Cherokee County til 1230 PM. A tornado watch remains in effect for southeast sections of North Texas . . . generally southeast of a Fairfield-Longview-Marshall line til 4 PM . . . and a flash flood watch remains in effect for the same area til 600 PM.

At noon . . . NWS radar indicated a broken line of strong thunderstorms from near Marshall to Rusk and Crockett . . . moving southeast at 35 mph. The strongest storms were several miles northeast and south of Rusk. These storms have weakened during the past 30 minutes . . . although dime-size hail was reported by storm spotters in Jacksonville at 1145 AM.

There is a slight risk of severe thunderstorms redeveloping this evening and tonight over all of North Texas as another upper level disturbance moves across the area. The weather pattern favors large hail . . . damaging winds . . . and heavy rainfall . . . although isolated tornadoes cannot be ruled out. The greatest threat of severe weather appears to be near a rain-cooled outflow boundary . . . near an Abilene-Hamilton-College Station line at noon. The future location of this boundary is uncertain . . . although the approach of the upper system may cause the boundary to move slowly north. Storm spotters and emergency operating centers will be activated if severe thunderstorms occur later today and tonight.

Midafternoon surface charts and radar reports (not shown) and satellite images (Fig. 13) show thunderstorms moving into the Texas Panhandle, already having produced strong wind gusts. These storms are approaching the remnants of the morning's thunderstorm-induced outflow boundary. The boundary has begun to move north, as anticipated, in response to rapid pressure falls in the Panhandle, apparently induced by the advancing short-wave trough. Temperatures and dewpoints have risen considerably near the boundary [e.g., Waco's temperature/dewpoint rose from 70/66°F (21/19°C) at 1800 UTC to 85/73°F (29/23°C) at 2100 UTC]. Small cumulus clouds have formed near the outflow boundary and the stationary

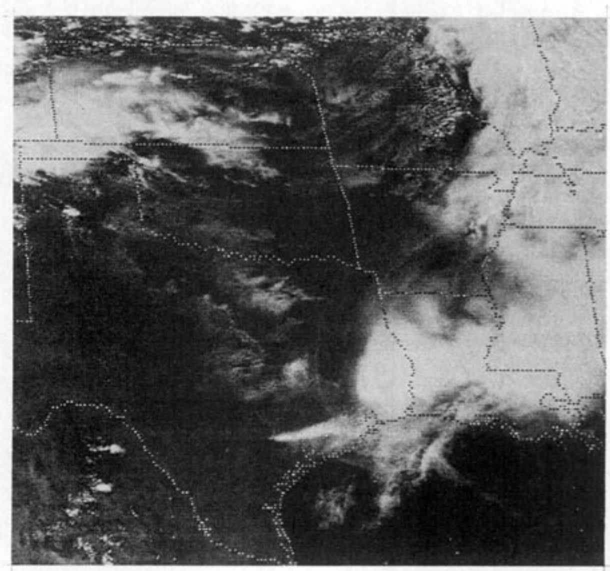

FIG. 13. Visible GOES image at 2031 UTC.

front to the north (Figs. 9 and 13), with an isolated thunderstorm developing along the boundary in the southern Panhandle.

Although the midafternoon ground-relative winds have remained light across the Panhandle and north Texas, the thunderstorms have accelerated in their forward motion across northwest Texas, with individual cells moving southeast (from 310°) at 25 m s^{-1}. Therefore, the *storm-relative* low-level winds have become quite strong and it is likely that the storm-relative helicity has increased as well. Considering the probable helicity increase and the ongoing destabilization, the Severe Local Storm Forecast Center (SELS) issues a tornado watch at 2030 UTC for the Panhandle.[9] Taking these factors into account, we (hypothetically) release a Severe Weather Outlook Statement at 2100 UTC.

> Severe Weather Outlook Statement
> National Weather Service Forecast Office, Ft Worth, TX
> Issued: 400 PM CDT May 4 1989
>
> The severe thunderstorm threat has been upgraded to a moderate risk this evening and tonight for that portion of North Texas south of a Bonham-Atlanta line. There is a slight risk of severe thunderstorms north of this line.
>
> An approaching upper air disturbance and surface cold front have combined with an unstable atmosphere to trigger severe thunderstorms across the Texas Panhandle this afternoon . . . with a tornado watch in effect for that area. Further southeast . . . an old rain-cooled outflow boundary was pushing north as a warm front through North Texas . . . causing atmospheric instabilities to increase. At 400 PM the boundary was situated near an Amarillo-Throckmorton-20 miles north of Waco line. The boundary was moving north at 20 mph on the west end and 10 mph on the east end.
>
> Atmospheric conditions are such that large hail . . . damaging winds . . . heavy rainfall . . . and a few tornadoes are possible tonight. The greatest threat of severe weather will be in the vicinity of the northward-moving warm front . . . particularly where the warm front intersects the advancing cold front. The threat has been upgraded to a moderate risk because of the rapidly increasing instabilities and an expected increase in vertical wind shear this evening.
>
> Activation of storm spotters and emergency operating centers is likely this evening and tonight as the current Panhandle thunderstorms move southeast into North Texas.

Our confidence level is increasing that thunderstorms (and some severe weather) will occur during the night in north Texas. Therefore, we augment office staffing levels (calling in extra help, if necessary) to ensure that we can handle the additional workload of weather warning and severe storm/flash flood potential analysis (hourly surface map analysis, radar analysis, storm spotter activation, etc.).

The 0000 UTC SEP sounding (Fig. 14a) confirms that the atmosphere has become quite unstable, with a CAPE of 4859 J kg^{-1} (lifted index of −10 at 500 mb) for a surface parcel. On the other hand, the hodograph shows weak low-level (ground relative) winds, which might indicate low supercell potential (Droegemeier et al. 1993). Using the SHARP program's algorithm for *estimating* storm motion gives quite low storm-relative helicity values (less than 50 $m^2 s^{-2}$). Having contours of helicity on the hodograph, however, allows us to estimate the helicity, which is around 215 $m^2 s^{-2}$ using the *observed* storm motion (Fig. 14b), a substantial value (see DBF90) but still somewhat smaller than in the morning. The BRN value is 85, based on the observed sounding at 0000 UTC, which is outside the range wherein supercells are likely (i.e., 10–40; as noted in section 3e).

Further, hourly surface observations reveal extreme pressure falls and low-level wind accelerations ahead of the Panhandle storms as they enter north Texas. Childress (CDS) exhibits a 3-h surface pressure fall of 6.6 mb and a 1-h drop of 2.9 mb (Fig. 15)! The pressure falls have resulted in increased surface winds at CDS, undoubtedly increasing helicity values.[10] It is not surprising that the Panhandle storms organize into a bow echo and attendant mesolow (Figs. 16 and 17), and produce a derecho (Johns and Hirt 1987), considering the large amounts of instability and vertical wind shear (Weisman 1992, 1993), as well as the presence of the thermal boundary (with its rich source of low-level moisture convergence, vorticity, and warm advection) and the strength of the approaching midlevel jet.

A tornado watch is issued for much of the North Texas area as the developing bow-echo complex approaches. At this transitional time we change our public statement strategy from that of the forecast (severe weather outlook) to a very short range forecast (or nowcast) in the form of special weather statements.

> Special Weather Statement
> National Weather Service Fort Worth TX
> 800 pm CDT Thu May 04 1989
>
> . . . Tornado watch issued as severe storms move into North Texas . . .
>
> A tornado watch is in effect for all but extreme southeast portion of North Texas til 200 am Friday morning.
>
> At 800 pm . . . radar indicated a short line of severe thunderstorms about 50 miles west of Wichita Falls. These storms were moving rapidly southeast at 50 mph.

[9] This watch actually was issued.

[10] The large pressure falls and low-level wind response probably resulted in part from upper-air divergence (and its associated upward motion) in the left-forward quadrant of a pronounced mid- and upper-level jet streak digging into the Texas panhandle.

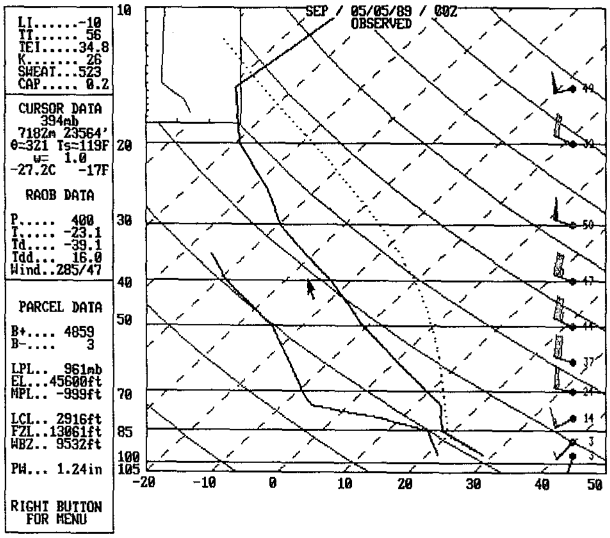

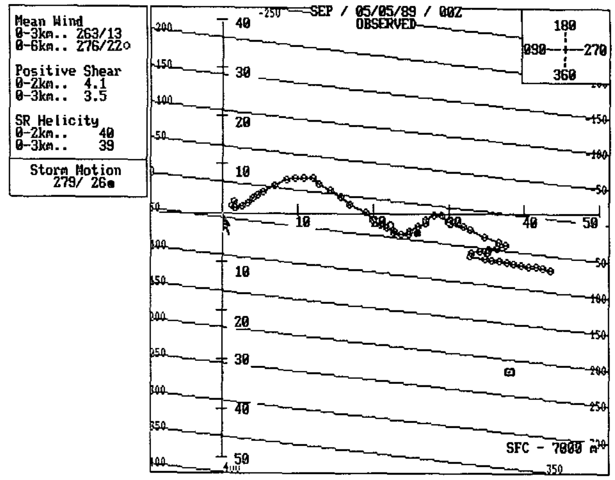

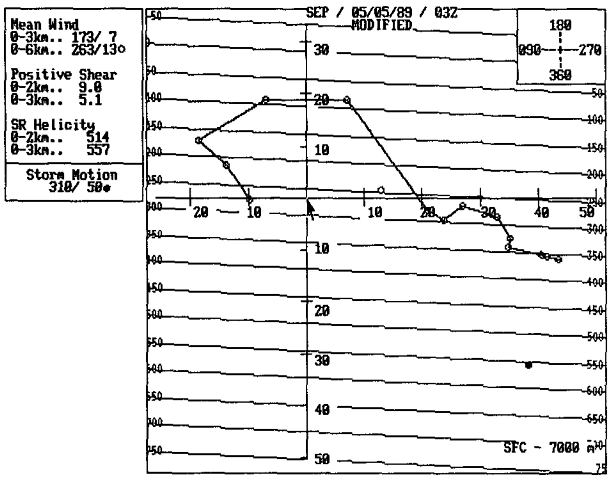

FIG. 14. Sounding (a), including (dotted line) an ascent curve for a surface parcel, and hodograph (b) at 0000 UTC 5 May 1989 from Stephenville, as in Fig. 11, with helicity calculations using a storm motion of 30° to the right at 75% of the speed of the 0–6-km mean wind (solid dot). The observed storm motion from 310° at 25 m s^{-1} is also plotted on the hodograph (denoted by the small dot inside the small rectangle). Also, an estimated hodograph (c) at 0300 UTC for the Fort Worth area, just ahead of the advancing storm cell D; storm-relative helicity calculations are done using the observed storm motion, and the hodograph is plotted with winds at 500-m intervals.

> The configuration of the thunderstorm line and the extremely unstable atmosphere ahead of it indicate a high likelihood of severe weather . . . especially large hail . . . very damaging winds . . . and a few tornadoes. This has been substantiated by spotter reports of 80 mph winds and baseball-size hail in rural Foard and Knox counties.
>
> Assuming that these storms maintain their intensity and forward motion . . . severe weather can be expected in Stephens and Palo Pinto counties by 900 pm . . . and Eastland and Erath counties by 930 pm.

The derecho-producing bow-echo complex moves into the Fort Worth County Area of Responsibility (CAR) shortly before 0200 UTC. The approach of the bow-echo MCS alone is cause for great concern of possible widespread downburst damage. The presence of classic and HP supercell-like structures within the bow-echo system (Figs. 16 and 17) suggests that large hail and tornadoes may accompany the downbursts, adding significantly to the overall threat to life and property.

We issue the first of many warnings at 0152 UTC, noting the reports of 7-cm diameter hail, wind gusts of 45 m s^{-1}, several tornadoes in the Abilene (ABI) and Wichita Falls (SPS) CARs, and the supercell structures within the bow-echo system. (Compare the echo mass shapes in Fig. 4 to those of individual cells embedded within the convective complex, especially near and north of the bow in Figs. 16 and 17.)

> Severe Thunderstorm Warning
> National Weather Service Fort Worth TX
> 852 pm CDT Thu May 04 1989
>
> The National Weather Service has issued a severe thunderstorm warning valid til 930 pm CDT for people in the following counties . . .
>
> In North Central Texas . . Stephens . . .

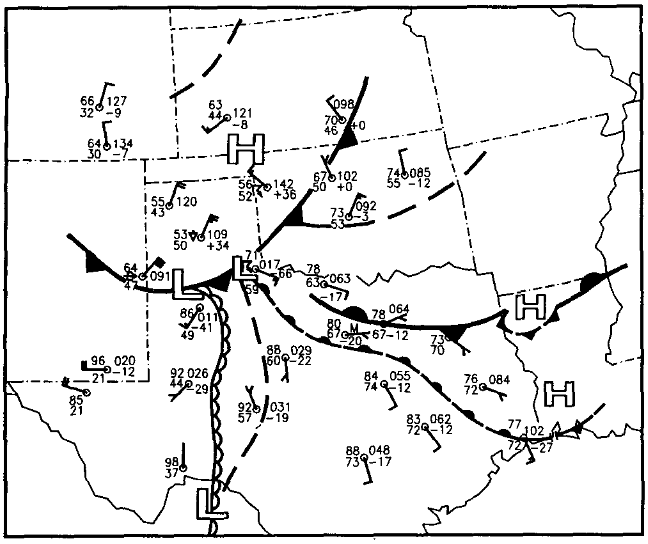

FIG. 15. As in Fig. 9 except at 0000 UTC.

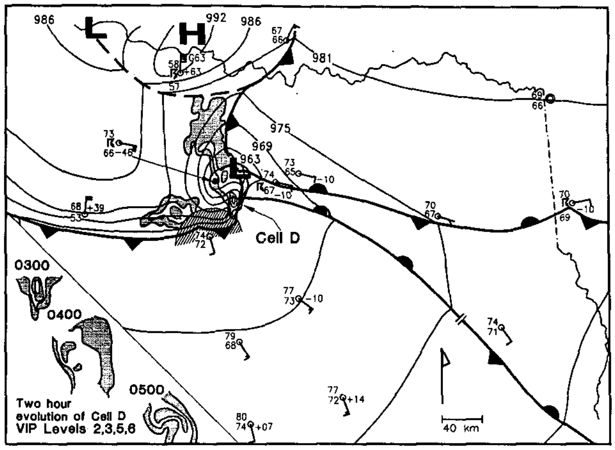

FIG. 16. Analysis of surface data at 0300 UTC, showing the outflow from the thunderstorms moving along the old front and outflow boundary in north Texas. Radar echoes at VIP levels 2, 3, 5, and 6 are shown at 0300 UTC on the analysis, with the inset showing the echo evolution of cell D at hourly intervals at 0300, 0400, and 0500 UTC.

At 850 pm . . . radar indicated severe thunderstorms along an arcing line from 30 miles southwest of Wichita Falls to Graham and 40 miles north of Abilene. The thunderstorms were moving southeast at 55 mph. Baseball-size hail . . . several tornadoes . . . and 85 mph wind gusts have been reported with these storms. Stephens County residents should seek interior shelter immediately as very damaging winds and large hail are imminent during the next 40 minutes.

The initial warning is followed by a nowcast of where the greatest severe weather threat is expected during the next several hours. Our analysis of the vertical wind shear and the extreme instability convinces us that the MCS will be long lived (Weisman 1992, 1993). We want to convey to the public that the system will continue into the densely populated Dallas–Fort Worth metropolitan area.

Severe Weather Statement
National Weather Service Fort Worth TX
910 pm CDT Thu May 04 1989

. . . Severe thunderstorm warning for Stephens county remains in effect til 930 pm. Severe storms approaching Palo Pinto . . . Parker . . . Hood . . . Erath . . . and Tarrant counties.

At 910 pm . . . a very dangerous line of thunderstorms extended from south of Wichita Falls to Breckenridge and northeast of Abilene. A severe thunderstorm warning for Palo Pinto county will be issued within minutes. Meteorological conditions are such that this dangerous line of thunderstorms should continue to move very rapidly southeast into the Dallas-Fort Worth . . . Mineral Wells . . . Weatherford . . . and Stephenville areas during the next several hours. Storm spotters should be activated . . . and residents in these areas should be ready to take necessary precautions when warnings are issued.

A tornado watch remains in effect til 200 AM CDT Friday morning for all but the extreme northwest and the extreme southeast sections of North Texas.

Severe storm spotter reports arrive and warnings are issued quickly during the next several hours. The extra "mesoscale desk" forecaster adjusts the 0000 UTC helicity estimates, based on a surface report at 0300 UTC of east winds at 5 m s^{-1} (10 kt) at the Dallas–Fort Worth airport (DFW) and a visual observation of low-level stratus clouds moving rapidly northwest (an estimated 600-m-AGL wind from 120° at 10 m s^{-1}). This increases the storm-relative, 0–3-km helicity estimate from more than 200 m^2 s^{-2} (at 0000 UTC) to

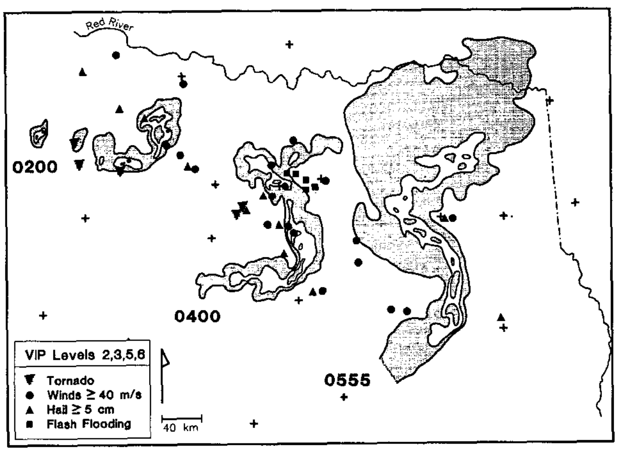

FIG. 17. Echo evolution over north Texas from 0200 to 0555 UTC, with significant severe weather reports (see the key) plotted. Hail sizes given refer to diameters.

more than 550 $m^2 s^{-2}$ (see Fig. 14c). Also, the BRN value decreases from 85 to 45, which is still outside the preferred range but could now be considered marginally favorable for supercells. These figures and the spotter reports of numerous *significant* severe weather events (as defined by Hales 1988), as well as the radar imagery (see Fig. 17), all confirm the likelihood of supercells with some of the storms in the bow-echo complex.

Shortly before 0300 UTC, a possible hook echo is observed about 60 km northeast of SEP, near the edge of the ground clutter, with storm "D" (Fig. 16). A check with the SEP radar operation confirms that the hook is bona fide, since it is located beneath a BWER. We issue a tornado warning for Hood County.

> Tornado Warning
> National Weather Service Fort Worth TX
> 1003 pm CDT Thu May 04 1989
>
> The National Weather Service has issued a tornado warning valid til 1045 pm CDT for people in the following counties . . .
>
> In North Texas . . . Hood . . .
> At 1000 pm . . . radar indicated a possible tornado about 3 miles north of Granbury . . . moving southeast at 50 mph. Golfball hail was falling in the same area at 1000 pm. Residents near Granbury Lake . . . and rural areas east of Granbury should take shelter in a reinforced structure immediately.

Additional warnings and statements are issued, keying on the multiple threats from the supercell-producing complex. In spite of the fast movement of the storms, a combined severe thunderstorm–flash flood warning is issued for the Dallas–Fort Worth metroplex.[11] The substantial rains associated with HP supercells, in conjunction with rapid runoff typical in urban areas, make flash flooding a real threat in the metropolitan area. The following statement summarizes the situation at 0320 UTC.

> Severe Weather Statement
> National Weather Service Fort Worth TX
> 1020 pm CDT Thu May 04 1989
>
> . . . Life threatening storm moving across North Texas . . .
>
> Damaging tornadoes were reported at Possum Kingdom Lake at 940 pm and at Lake Granbury at 1013 pm. Tornado warnings for Hood and Palo Pinto counties are in effect til 1045 pm. Residents in eastern portion of both counties should seek shelter in central portions of reinforced buildings or homes now. Cars and mobile homes should be abandoned for reinforced shelter.
>
> Severe thunderstorm warnings remain in effect for Johnson . . . Parker . . . Erath . . . and Somervell counties til 1100 pm. A combined severe thunderstorm and flash flood warning is in effect till 1120 pm for Tarrant county. Damaging winds and large hail are likely in these counties . . . and flash flooding is possible in urban areas of Tarrant county.
>
> At 1015 pm . . . radar and spotters indicated a line of severe thunderstorms from 10 miles west of Bridgeport to Weatherford . . . Granbury . . . and Stephenville. This unusually dangerous and fast-moving thunderstorm complex was traveling southeast at 60 mph.
>
> Residents of Dallas . . . Ellis . . . and Navarro counties can expect severe thunderstorm warnings within the next 30 minutes.

Severe weather events continue as the complex moves toward the Louisiana border during the next several hours (Fig. 17). Because of the SWOs and numerous statements and warnings, emergency management officials and spotters are at a high level of vigilance. Their reports, as well as additional NWS warnings and statements, are disseminated quickly downstream of the events by the news media and NOAA Weather Radio. When the intense convective system exits the FTW CAR, relevant information is phoned to downstream NWS warning offices.

Finally, a postevent study is initiated with the following objectives: 1) determine if (and how) forecast office procedures and actions could have been improved during the event, 2) learn about the meteorological environment that produced the intense convective system, and 3) summarize severe event locations and times to compare to radar imagery and to include in *Storm Data*.

Analysis of radar film indicated at least six different supercell storms while the complex was in north Texas. Five of the six exhibited at least one transition from HP or classic supercell to bow-echo cell structure, similar to cell D in Fig. 16. (Analysis of the sixth supercell's life cycle was interrupted by a lapse in the radar film.) Supercell D completed its transition from classic supercell to bow echo 2 h after first exhibiting supercell structure, whereas the other cells underwent similar transitions in less than 1.5 h.

There were approximately 175 wind and hail reports and 5 tornadoes with the bow-echo system. Twenty-nine of the hail and wind reports were significant (Figs. 16 and 17). Ten of 11 significant hail events, 14 of 18 significant wind reports, and 3 of 5 tornadoes occurred with the 6 supercell storms, clearly indicating the importance of recognizing and warning for these storms. All of the significant hail events and tornadoes occurred prior to the supercell to bow-echo transition. The 14 significant wind events were evenly split between supercell and bow-echo cell stages. There were 5 flash flood deaths (all in the Dallas–Fort Worth area), 1 downburst death, 22 tornado injuries (all in Hood

[11] The 1989 derecho followed the pattern of a 1976 event that moved along a similar track. As in the 1976 derecho, storms north of the primary bow position underwent a classic-to-HP supercell transition, producing flash flooding and damaging winds during their HP stages (Moller et al. 1990).

County), and 10 downburst injuries in north Texas. Damage approached $100 million.

5. Summary and discussion

Numerical modeling and operational considerations have suggested that a supercell storm be defined as one with a mesocyclone (vertical component of relative vorticity $\geq 10^{-2}\ s^{-1}$) that persists at least on the order of tens of minutes and is present through a substantial fraction ($\geq 1/3$) of the convective storm's depth. Supercells are rare relative to other storm types, even during the spring in the American Great Plains. Nevertheless, they produce a disproportionately large amount of thunderstorm-caused casualties and damage. Therefore, it is essential for the NWS to detect and warn for them, regardless of where and when they occur. Just as a successful forecast should be made for an extremely rare snow event in south Florida, a supercell outbreak in upper New England or California should not elude the NWS watch/warning program.

Forecasters should have the tools and knowledge not only to detect supercell storms but also to diagnose the atmospheric conditions that favor their occurrence. An understanding of the multiscale meteorological interactions that result in supercells allows the forecaster to maximize the number of detected supercell events while minimizing the number of false alarms. Forecasters should understand that the different scales of motion are not independent of each other in a supercell (or any other) forecast situation. Synoptic-scale processes strongly influence the evolution of mesoscale systems (Anthes et al. 1982) that, in turn, affect the convection; feedbacks also go the opposite way (upscale).

When considering supercell environments, forecasters should use a two-stage procedure in answering questions about supercell potential (see also Johns and Doswell 1992). First, forecasters should determine the temporal and spatial limits of deep, moist convection through an accurate diagnosis of moisture, instability, and mesoscale lifting mechanisms. The second step is to ascertain where and when within the convective forecast area the combination of vertical wind shear and CAPE is conducive for mesocyclones. Using the BRN can give forecasters a rough idea of supercell potential, subject to the limitation that it can be assessed only at sounding times. Monitoring the vertical wind shear, particularly as evaluated in the form of storm-relative 0–3-km helicity, is crucial for determining mesocyclone potential as the situation evolves. Rapid temporal and spatial changes in helicity from hour to hour dictate a close weather watch and constant updating based on changing wind conditions and observed storm motions.

In the pre-WSR-88D NWS office, supercell detection can be accomplished by judicious use of both volumetric radar observations and severe storm spotters. Low-level plan position indicator radar signatures of storm structures, such as possible hook echoes, should be verified by the presence of features above the hook (BWERs, WERs, etc.) that confirm the presence of a powerful updraft and by the exhibition of temporal continuity over a period of minutes of "distinctive" features (e.g., hook and bow echoes). Storm spotter reports of persistent rotating wall clouds with strong, warm inflow mean that a storm's three-dimensional reflectivity structure should be analyzed carefully, regardless of whether or not a hook- or pendant-shaped low-level signature is observed.

Furthermore, NWS forecasters should be wary of different arrangements of radar reflectivity patterns in and adjacent to the mesocyclone. "Nonclassic" supercells may have considerable precipitation falling in the mesocyclone itself (HP supercell characteristics), such that the radar and visual appearances can be difficult to interpret. The mesocyclone may occur more toward the front flank, relative to storm motion, than on the "classic" right-rear storm flank, with the echo exhibiting a front-flank inflow notch or even a bow-echo shape. Low-precipitation supercells generally have very little precipitation in the mesocyclone and in the main body of the storm's reflectivity echo, rendering radar detection very difficult. Nevertheless, storm spotters may observe an updraft with very obvious rotation; such storms are capable of producing giant hail and tornadoes.

6. Supercell forecasting and detection in the modernized and restructured NWS

The knowledgeable forecaster will benefit greatly from the advanced datasets available in the MAR NWS. For instance, critical changes in vertical wind profiles (and helicity) will be easier to detect with profilers and the WSR-88D algorithm known as Velocity Azimuth Display (VAD). Another WSR-88D algorithm will calculate storm motion, the other variable in the helicity calculation, with more accuracy than the current subjectively estimated technique.

Computer upgrades in the NWS national centers (class VII computers with a tenfold increase of computing power) and in local offices (e.g., deployment of the Advanced Weather Interactive Processing System, and personal computers) offer a promise of smooth, high-resolution data flow. These data include the eventual implementation of enhanced satellite imagery, high-density Automated Surface Observing Systems, and gridded model output data (for local analysis of diagnostic products derived from model forecasts) from high-resolution numerical models such as the Mesoscale Analysis and Prediction System (see NOAA staff 1990). All of this will aid in improving multiscale analysis, again assuming that the forecaster learning curve keeps pace with technological advances.

The most powerful tool, by far, in the MAR NWS for supercell detection will be the WSR-88D radar and display system. The high-resolution, extensive WSR-88D data will provide knowledgeable forecasters with superior visualization of three-dimensional thunderstorm structure and circulation, allowing easier identification of convective storm type. Through judicious use of these radar data, forecasters will be able to determine which storms are the most viable candidates to produce mesocyclones, even *before* Doppler velocities indicate rotation. This will allow forecasters to issue timely, prewarning nowcasts for emergency preparedness and storm spotter purposes. Time constraints during a major supercell outbreak are such that *forecasters should have a more aggressive warning attitude than one of waiting for Doppler velocity-detected mesocyclone formation.* Certainly, once serious weather events such as killer tornadoes have occurred, meteorologists should determine quickly which storms are evolving similarly to the initial tornadic storms (through close examination of three-dimensional reflectivity and velocity data) and initiate warnings (F. Makosky 1991, personal communication).

Doppler velocity base data and mesocyclone algorithms[12] are the most critical WSR-88D supercell-detection products available to forecasters. Nevertheless, in spite of the superiority of WSR-88D data, storm structures at great range will be difficult to detect. Specifically, mesocyclones will be hard to identify beyond 200 km because of the radar horizon[13] and the so-called aspect ratio problem—that is, when the radar resolution volume size becomes significantly larger (about a factor of 3 for a Rankine combined vortex, according to Burgess and Lemon 1990) than the mesocyclone radius. Forecasters will have to rely on conceptual storm model knowledge to interpret WSR-88D reflectivity and velocity data, storm spotter reports, and satellite imagery properly when outright mesocyclone detection is impossible (Jones et al. 1985) or when mesocyclone algorithms produce occasional false alarms. Further, when a tornadic storm moves out of optimal range for detecting low-level features, if it remains a strong storm, it should be treated as a tornadic storm. Spotters may be very important in such cases.

Furthermore, sound knowledge of supercell storms and their environments will be an absolute necessity in using the WSR-88D effectively. Foster (1990) has shown that the copious amount of WSR-88D data makes it imperative that meteorologists specify ahead of time which products will be included on a given day in the Routine Products Set, since the system (and the forecaster) can be overloaded quickly. To accomplish this, forecasters must *anticipate* the meteorological events (such as supercells, nontornadic thunderstorms, flash flooding, etc.) that are possible on that particular day.

Finally, the use of VAD wind profiles from the WSR-88D system will allow the monitoring of the evolving environment, which we believe is a crucial part of detection. Anticipating supercells by monitoring the SREH using VAD wind profiles (and other techniques) is a critical part of recognizing supercells when they develop.

In closing, we wish to emphasize that coping with supercell events in operations will depend on forecasters having adequate knowledge of supercell conceptual models even as new technologies are implemented. We have introduced the idea of a supercell spectrum as an aid to recognition of supercells because many storms with mesocyclones do not have echo morphologies that match traditional supercell models in the literature. Even though Doppler radars will make mesocyclone detection more reliable than at present, it is important operationally to be able to anticipate supercells before they develop. Taking full advantage of the new tools will require forecasters to master the tools available at present. Thus, understanding of what environments favor supercells is also crucial. We have indicated what is possible even with today's technology; we look forward to what will be possible with the technology that will be available in the modernized and restructured NWS.

Acknowledgments. We are grateful to Ms. Joan O'Bannon for her help in drafting the figures and to Mr. John Hart for his assistance with the SHARP program. Critical reviews by Mr. R. H. Johns and an anonymous referee were helpful in improving the presentation. Drs. Harold Brooks and Robert Davies-Jones provided many insightful discussions.

REFERENCES

Anthes, R. A., Y. H. Kuo, S. G. Benjamin, and Y. F. Li, 1982: The evolution of the mesoscale environment of severe local storms: Preliminary modeling results. *Mon. Wea. Rev.*, **110**, 1187–1213.

Bluestein, H. B., and C. R. Parks, 1983: A synoptic and photographic climatology of low-precipitation severe thunderstorms in the Southern Plains. *Mon. Wea. Rev.*, **111**, 2034–2046.

——, and G. R. Woodall, 1990: Doppler-radar analysis of a low-precipitation severe storm. *Mon. Wea. Rev.*, **118**, 1640–1664.

Braun, S. A., and J. P. Monteverdi, 1991: An analysis of a mesocyclone-induced tornado occurrence in northern California. *Wea. Forecasting*, **6**, 13–31.

Brooks, E. M., 1949: The tornado cyclone. *Weatherwise*, **2**, 32–33.

Brooks, H. E., and R. B. Wilhelmson, 1992: Numerical simulation of a low-precipitation supercell thunderstorm. *Meteor. Atmos. Phys.*, **49**, 3–17.

——, C. A. Doswell III, and R. Davies-Jones, 1993: Environmental helicity and the maintenance and evolution of low-level mesocyclones. *The Tornado: Its Structure, Dynamics, Prediction,*

[12] Users of the algorithms should be aware that they will be in a state of development for a number of years to come, with the aim being to increase the detection rate and decrease the *false* detection rate. As this improvement occurs, the value of the algorithms should increase accordingly.

[13] This problem is exacerbated when the convection has low tops.

and Hazards. Geophys. Monogr., No. 79, Amer. Geophys. Union, 97–104.

——, ——, and R. B. Wilhelmson, 1994: The role of midtropospheric winds in the evolution and maintenance of low-level mesocyclones. *Mon. Wea. Rev.*, **122**, 126–136.

Browning, K. A., 1964: Airflow and precipitation trajectories within severe local storms which travel to the right of the winds. *J. Atmos. Sci.*, **21**, 634–639.

Burgess, D. W., 1988: The environment of the Edmond, Oklahoma, tornadic storm. Preprints, *15th Conf. Severe Local Storms*, Baltimore, MD, Amer. Meteor. Soc., 292–295.

——, and R. P. Davies-Jones, 1979: Unusual tornadic storms in eastern Oklahoma on 5 December 1975. *Mon. Wea. Rev.*, **107**, 451–457.

——, and E. B. Curran, 1985: The relationship of storm type to environment in Oklahoma on 26 April 1984. Preprints, *14th Conf. Severe Local Storms*, Indianapolis, IN, Amer. Meteor. Soc., 208–211.

——, and L. R. Lemon, 1990: Severe thunderstorm detection by radar. *Radar in Meteorology*, D. Atlas, Ed., Amer. Meteor. Soc., 619–647.

——, V. T. Wood, and R. A. Brown, 1982: Mesocyclone evolution statistics. Preprints, *12th Conf. on Severe Local Storms*, San Antonio, TX, Amer. Meteor. Soc., 422–424.

Byers, H. R., 1942: Nonfrontal thunderstorms. Miscellaneous Report No. 3, University of Chicago Press, 26 pp.

Carlson, T. N., S. G. Benjamin, G. S. Forbes, and Y. F. Li, 1983: Elevated mixed layers in the regional severe storm environment: Conceptual model and case studies. *Mon. Wea. Rev.*, **111**, 1453–1473.

Charba, J. P., and Y. Sasaki, 1971: Structure and movement of the severe thunderstorms of 3 April 1964 as revealed from radar and surface mesonetwork data analysis. *J. Meteor. Soc. Japan*, **49**, 191–214.

Chisolm, A. J., and J. H. Renick, 1972: The kinematics of multicell and supercell Alberta hailstorms. Alberta Hail Studies, 1972, Research Council of Alberta Hail Studies Report No. 72-2, 24–31.

Davies-Jones, R. P., D. W. Burgess, and M. Foster, 1990: Test of helicity as a tornado forecast parameter. Preprints, *16th Conf. on Severe Local Storms*, Kananaskis Park, Alberta, Canada, Amer. Meteor. Soc., 588–592.

Dessens, J., and J. T. Snow, 1989: Tornadoes in France. *Wea. Forecasting*, **4**, 110–132.

Donaldson, R. J., Jr., 1970: Vortex signature recognition by a Doppler radar. *J. Appl. Meteor.*, **9**, 661–670.

Doswell, C. A., III, 1985: The operational meteorology of convective weather. Vol. II: Storm scale analysis. NOAA Tech. Memo. ERL ESG-15, 240 pp. [Available from National Severe Storms Laboratory, 1313 Halley Circle, Norman, OK 73069.]

——, 1987: The distinction between large-scale and mesoscale contribution to severe convection: A case study example. *Wea. Forecasting*, **2**, 3–16.

——, 1991: A review for forecasters on the application of hodographs to forecasting severe thunderstorms. *Natl. Wea. Dig.*, **16**, 2–16.

——, and H. E. Brooks, 1993: Comments on "Anomalous cloud-to-ground lightning in an F5-producing supercell thunderstorm on 28 August 1990." *Bull. Amer. Meteor. Soc.*, **74**, 2213–2218.

——, F. Caracena, and M. Magnano, 1985: Temporal evolution of 700–500 mb lapse rate as a forecasting tool—A case study. Preprints, *14th Conf. on Severe Local Storms*, Indianapolis, IN, Amer. Meteor. Soc., 398–401.

——, A. R. Moller, and R. Przybylinski, 1990: A unified set of conceptual models for variations on the supercell theme. Preprints, *16th Conf. on Severe Local Storms*, Kananaskis Park, Alberta, Canada, Amer. Meteor. Soc., 40–45.

Droegemeier, K. K., S. M. Lazarus, and R. Davies-Jones, 1993: The influence of helicity on numerically simulated convective storms. *Mon. Wea. Rev.*, **121**, 2005–2029.

Fankhauser, J. C., and C. G. Mohr, 1977: Some correlations between various sounding parameters and hailstorm characteristics in northeast Colorado. Preprints, *10th Conf. on Severe Local Storms*, Omaha, NE, Amer. Meteor. Soc., 218–225.

Foote, G. B., and H. W. Frank, 1983: Case study of a hailstorm in Colorado. Part III: Airflow from triple Doppler measurements. *J. Atmos. Sci.*, **40**, 686–706.

Forbes, G. S., 1981: On the reliability of hook echoes as tornado indicators. *Mon. Wea. Rev.*, **109**, 1457–1466.

Foster, M., 1990: NEXRAD operational issues: Meteorological considerations in configuring the radar. Preprints, *16th Conf. on Severe Local Storms*, Kananaskis Park, Alberta, Canada, Amer. Meteor. Soc., 189–192.

Fujita, T. T., 1960: A detailed analysis of the Fargo tornadoes of June 20, 1957. U.S. Weather Bureau Research Paper No. 42, 67 pp.

——, D. L. Bradbury, and C. F. Van Thullenar, 1970: Palm Sunday tornadoes of April 11, 1965. *Mon. Wea. Rev.*, **98**, 29–69.

Hales, J. E., 1988: Improving the watch/warning program through use of significant event data. Preprints, *15th Conf. on Severe Local Storms*, Baltimore, MD, Amer. Meteor. Soc., 165–168.

Hart, J. A., and W. D. Korotky, 1991: *The SHARP Workstation—v1.50. A Skew T/Hodograph Analysis and Research Program for the IBM and Compatible PC. User's Manual.* NOAA/NWS, 62 pp.

Imy, D. A., K. J. Pence, and C. A. Doswell III, 1992: On the need for volumetric radar data when issuing severe thunderstorm and tornado warnings. *Natl. Wea. Dig.*, **17**, 2–17.

Johns, R. H., 1993: Meteorological conditions associated with bow echo development in convective storms. *Wea. Forecasting*, **8**, 294–299.

——, and W. D. Hirt, 1987: Derechos: Widespread convectively induced windstorms. *Wea. Forecasting*, **2**, 32–49.

——, and C. A. Doswell III, 1992: Severe local storms forecasting. *Wea. Forecasting*, **7**, 588–612.

——, J. M. Davies, and P. W. Leftwich, 1993: Some wind and instability parameters associated with strong and violent tornadoes. Part II: Variations in the combinations of wind and instability parameters. *The Tornado: Its Structure, Dynamics, Prediction, and Hazards, Geophys. Monogr.*, No. 79, Amer. Geophys. Union, 583–590.

Jones, W. A., K. K. Keeter, and L. L. Lee, 1985: Some considerations for long-range radar evaluation of potentially tornadic thunderstorms. Preprints, *14th Conf. on Severe Local Storms*, Indianapolis, IN, Amer. Meteor. Soc., 139–142.

Klemp, J. B., 1987: Dynamics of tornadic thunderstorms. *Ann. Rev. Fluid Mech.*, **19**, 369–402.

Korotky, W. D., 1990: The Raleigh tornado of November 28, 1988: The evolution of the tornadic environment. Preprints, *16th Conf. on Severe Local Storms*, Kananaskis Park, Alberta, Canada, Amer. Meteor. Soc., 532–537.

Lemon, L. R., 1980: Severe thunderstorm radar identification techniques and warning criteria: A preliminary report. NOAA Tech. Memo. NWS NSSFC-1, 60 pp. [NTIS PB273049.]

——, and C. A. Doswell III, 1979: Severe thunderstorm evolution and mesocyclone structure as related to tornadogenesis. *Mon. Wea. Rev.*, **107**, 1184–1197.

Maddox, R. A., 1993: Diurnal low-level wind oscillation and storm-relative helicity. *The Tornado: Its Structure, Dynamics, Prediction, and Hazards, Geophys. Monogr.*, No. 79, Amer. Geophys. Union, 591–598.

——, and C. A. Doswell III, 1982: An examination of jet stream configurations, 500 mb vorticity advection, and low-level thermal advection patterns during extended periods of intense convection. *Mon. Wea. Rev.*, **110**, 184–197.

——, L. R. Hoxit, and C. F. Chappell, 1980: A study of tornadic thunderstorm interactions with thermal boundaries. *Mon. Wea. Rev.*, **108**, 322–336.

Marwitz, J. D., 1972: The structure and motion of severe hailstorms. Part II: Multi-cell storms. *J. Appl. Meteor.*, **11**, 180–188.

McCaul, E. W., Jr., 1991: Buoyancy and shear characteristics of hurricane–tornado environments. *Mon. Wea. Rev.*, **119**, 1954–1978.

Miller, R. C., 1972: Notes on analysis and severe-storm forecasting procedures of the Air Force Global Forecast Center. Air Weather Service Tech. Rep. 200 (rev.), Air Weather Service Headquarters, Scott Air Force Base, IL, 190 pp.

Moller, A. R., 1978: The improved NWS storm spotter's training program at Ft. Worth, TX. *Bull. Amer. Meteor. Soc.*, **59**, 1574–1582.

——, C. A. Doswell III, and R. Przybylinski, 1990: High-precipitation supercells: A conceptual model and documentation. Preprints, *16th Conf. on Severe Local Storms,* Kananaskis Park, Alberta, Canada, Amer. Meteor. Soc., 52–57.

Nelson, S. P., 1987: The hybrid multicellular-supercellular storm—An efficient hail producer. Part II: General characteristics and implications for hail growth. *J. Atmos. Sci.*, **44**, 2060–2073.

NOAA staff, 1990: National implementation plan for the modernization and associated restructuring of the national weather service. U.S. Government Printing Office 261-983/23426.

Nolen, R. H., 1959: A radar pattern associated with tornadoes. *Bull. Amer. Meteor. Soc.*, **40**, 277–279.

Penn, S., C. Pierce, and J. K. McGuire, 1955: The squall line and Massachusetts tornadoes of June 9, 1953. *Bull. Amer. Meteor. Soc.*, **36**, 109–122.

Przybylinski, R. W., 1988: Radar signatures associated with the 10 March 1986 tornado outbreak over central Indiana. Preprints, *15th Conf. on Severe Local Storms,* Baltimore, MD, Amer. Meteor. Soc., 253–256.

——, S. Runnels, P. Spoden, and S. Summy, 1990: The Allendale, Illinois tornado—January 7, 1989. One type of an HP supercell. Preprints, *16th Conf. on Severe Local Storms,* Kananaskis Park, Alberta, Canada, Amer. Meteor. Soc., 516–521.

Ray, P. S., R. J. Doviak, G. B. Walker, D. Sirmans, J. Carter, and B. Baumgarner, 1975: Dual-Doppler observations of a tornadic storm. *J. Appl. Meteor.*, **14**, 1521–1530.

Schlesinger, 1980: A three-dimensional numerical model of an isolated thunderstorm. Part II: Dynamics of updraft splitting and mesovortex couplet evolution. *J. Atmos. Sci.*, **37**, 396–420.

Smith, B. E., 1990: Mesoscale structure of a derecho-producing convective system: The Southern Great Plains storm of May 4, 1989. Preprints, *16th Conf. on Severe Local Storms,* Kananaskis Park, Alberta, Canada, Amer. Meteor. Soc., 455–460.

Vasiloff, S. V., E. A. Brandis, R. P. Davies-Jones, and P. S. Ray, 1986: An investigation of the transition from multicell to supercell storms. *J. Climate Appl. Meteor.*, **25**, 1022–1036.

Vescio, M. D., K. K. Keeter, P. Badgett, and A. J. Riordan, 1993: A low-top weak-reflectivity severe weather episode along a thermal/moisture boundary in eastern North Carolina. Preprints, *17th Conf. on Severe Local Storms,* St. Louis, MO, Amer. Meteor. Soc., 628–632.

Weaver, J. F., and S. P. Nelson, 1982: Multiscale aspects of thunderstorm gust fronts and their effects on subsequent storm development. *Mon. Wea. Rev.*, **110**, 707–718.

Wesiman, M. L., 1992: The role of convectively generated rear-inflow jets in the evolution of long-lived meso-convective systems. *J. Atmos. Sci.*, **49**, 1826–1847.

——, 1993: The genesis of severe, long-lived bow echoes. *J. Atmos. Sci.*, **50**, 645–670.

——, and J. B. Klemp, 1982: The dependence of numerically simulated convective storms on vertical wind shear and buoyancy. *Mon. Wea. Rev.*, **110**, 504–520.

——, and ——, 1984: The structure and classification of numerically simulated convective storms in directionally varying wind shears. *Mon. Wea. Rev.*, **112**, 167–170.

——, and H. B. Bluestein, 1985: Dynamics of numerically simulated LP storms. Preprints, *14th Conf. on Severe Local Storms,* Indianapolis, IN, Amer. Meteor. Soc., 267–270.

——, and J. B. Klemp, 1986: Characteristics of isolated convection. *Mesoscale Meteorology and Forecasting,* P. S. Ray, Ed., Amer. Meteor. Soc., 331–358.

Woodall, G. R., 1990: Qualitative analysis and forecasting of tornadic activity using storm-relative helicity. NOAA Tech. Memo. NWS SR-127, 57 pp. [NTIS PB90171372/AS.]